

Aus der Klinik für Orthopädie und Unfallchirurgie  
der Heinrich-Heine-Universität Düsseldorf

Direktor: Univ.-Prof. Dr. med. Joachim Windolf

Effects of non-thermal atmospheric pressure plasma on human  
fibroblasts

Dissertation

Zur Erlangung des Grades eines Doktors der Medizin  
der Medizinischen Fakultät der Heinrich-Heine-Universität  
Düsseldorf

vorgelegt von

Florian Jansen

2020

Als Inauguraldissertation gedruckt mit der Genehmigung der  
Medizinischen Fakultät der Heinrich-Heine-Universität Düsseldorf

gez.:

Dekan: Prof. Dr. med. Nikolaj Klöcker

Erstgutachter: Prof. Dr. rer. nat. Christoph V. Suschek

Zweitgutachter: PD Dr. rer. nat. Csaba Mahotka

*Für alle, von denen ich stetig lerne und mich zu einem besseren Menschen  
machen.*

## I. Summary

A promising approach to wound treatment is local application of non-thermal “cold” atmospheric plasma (CAP), which has a disinfectant effect. However, CAP can induce cellular toxicity, which could be a major disadvantage in wound treatment. In comparison to other CAP jets that use high gas flow (>3 slm), the micro-scaled Atmospheric Pressure Plasma Jet ( $\mu$ APPJ) can also be operated with a comparably low gas flow (0.25-1.40 slm), allowing the treatment of cells/tissue without excessive drying out and osmotic effects. Thus, we have studied the influence of  $\mu$ APPJ on human fibroblasts—the major cell type of the dermis crucial for successful skin healing—and CAP-induced physical/chemical changes of treated buffer. By CAP treatments (0.25 slm, 10 min) of 500  $\mu$ l PBS, a slight acidification ( $<0.2$ ), and the increase of nitrite ( $161 \pm 28 \mu\text{M}$ ), nitrate ( $352 \pm 60 \mu\text{M}$ ) and hydrogen peroxide ( $124 \pm 40 \mu\text{M}$ ) could be observed. Using a gas flow of 1.4 slm, CAP treatment (10 min) did not show a significant decrease in pH and induced lower accumulation of nitrite ( $44 \pm 7 \mu\text{M}$ ) and nitrate ( $10 \pm 2 \mu\text{M}$ ). However,  $\text{H}_2\text{O}_2$  concentrations ( $1265 \pm 149 \mu\text{M}$ ) and evaporation increased (50 % vs. 15 % using 0.25 slm). Direct and indirect CAP treatments of fibroblasts using 0.25 slm showed low toxicity (max. 20 %; 10 min). Due to the observed drying out effects, only indirect treatments using a gas flow of 1.40 slm were possible. Here, a 10 min CAP treatment followed by 5 min incubation with cells reduced viability ( $49 \pm 29 \%$  vs. untreated control), which could be prevented by the addition of catalase. By substitution of the evaporated water volume prior to the incubation with cells, the viability could be increased to  $66 \pm 19 \%$ . In addition, cell numbers determined 4 days after indirect CAP treatments were reduced by 29 % using 0.25 slm as well as by 42 % using 1.40 slm. These effects could be partially reversed by catalase, indicating that antiproliferative effects of CAP are induced by  $\text{H}_2\text{O}_2$  to a large extent. In summary, by operating the  $\mu$ APPJ with different gas flows, cell responses can be modulated via the accumulation of  $\text{H}_2\text{O}_2$ , nitrogen oxide derivatives (NOD), osmolarity and dry-out effects. In general, the  $\mu$ APPJ exerts low toxicity and only longer treatment periods influence cell viability and proliferation. Regarding the necessity of low gas flows and the sterilizing effects of the generated plasma, the  $\mu$ APPJ seems to be suitable for the treatment of dermal wounds.

# I. Zusammenfassung

Ein vielversprechender Ansatz Wunden zu behandeln ist die Anwendung von „kaltem“ Atmosphärendruckplasma (CAP), da es über ein breites antibakterielles Spektrum verfügt. CAP kann jedoch Zelltoxizität induzieren, was ein Rückschlag in der Wundforschung darstellen könnte. Im Vergleich zu anderen CAP Jets, welche über hohe Gasflussraten verfügen ( $>3$  slm), kann der micro-scaled Atmospheric Pressure Plasma Jet ( $\mu$ APPJ) mit einer niedrigeren Flussrate (0.25-1.4 slm) genutzt werden, sodass Gewebe/Zellen ohne ausgeprägte osmotische Effekte und Austrocknung behandelt werden könnten. Wir untersuchten den Einfluss des  $\mu$ APPJ auf humane Fibroblasten als dominierende Zellart der Haut, denen eine entscheidende Bedeutung in der Wundheilung zukommt, sowie die chemischen/physikalischen Veränderungen von behandeltem Buffermedium. Nach der Behandlung (0.25 slm, 10 min) von 500  $\mu$ l PBS zeigte sich eine Ansäuerung des pH-Wertes ( $<0.2$ ), ein Anstieg der Nitrit- ( $161 \pm 28 \mu\text{M}$ ), Nitrat- ( $352 \pm 60 \mu\text{M}$ ) und der  $\text{H}_2\text{O}_2$ -Konzentration ( $124 \pm 40 \mu\text{M}$ ). Unter 1.4 slm CAP-Behandlung (10 min) zeigte sich zwar keine signifikante Senkung des pH-Wertes und ein niedrigerer Anstieg der Nitrit- ( $44 \pm 7 \mu\text{M}$ ) und Nitratkonzentration ( $10 \pm 2 \mu\text{M}$ ), die  $\text{H}_2\text{O}_2$ -Konzentration ( $1265 \pm 149 \mu\text{M}$ ) und Verdunstung (50 % vs. 15 % bei 0.25 slm) stieg jedoch an. Die direkte und indirekte Behandlung von Zellen mit 0.25 slm zeigte eine niedrige Toxizität (max. 20 %; 10 min). Aufgrund der Austrocknung waren mit 1.4 slm nur indirekte Behandlungen möglich. Hier zeigte sich nach 10 min Behandlung gefolgt von 5 min Inkubationszeit eine reduzierte Viabilität ( $49 \pm 29$  % vs. Kontrolle), die durch Katalase aufgehoben werden konnte. Unter Substitution der Verdunstung vor der Inkubation stieg die Viabilität auf  $66 \pm 19$  %. 4 Tage nach indirekter CAP-Behandlung mittels 0.25 slm zeigte sich eine um 29 % und mittels 1.40 slm eine um 42 % reduzierte Zellzahl. Dieser Effekt konnte ebenfalls durch Katalase reduziert werden, sodass dieser vermutlich auf  $\text{H}_2\text{O}_2$  beruht. Somit lässt sich die Zellreaktion durch die Flussrate, die Akkumulation von  $\text{H}_2\text{O}_2$ , Stickstoffmonoxid-Derivaten (NOD), der Osmolarität und Austrocknung modulieren. Die Behandlung zeigte eine niedrige Toxizität und nur längere Behandlungszeiten beeinflussten die Viabilität und Proliferation. Bezogen auf die Notwendigkeit eines niedrigen Flussrate und der sterilisierenden Effekte des CAP ist der  $\mu$ APPJ ein geeignetes Gerät, um Wunden zu behandeln.

## II. Abbreviations

BSA	Bovine Serum Albumin
CAP	Cold Atmospheric Plasma
CLD	Chemiluminescence-Detection
DMEM	Dulbecco's Modified Eagle Medium
EDTA	Ethylenediaminetetraacetate
FCS	Fetal Calf Serum
HEPES	4-(2-hydroxyethyl)-1-piperazineethanesulfonic acid
HDF	Human Dermal Fibroblasts
$\mu$ APPJ	Micro-Scaled Atmospheric Pressure Plasma Jet
NO	Nitric Oxide
NO <sub>2</sub>	Nitrogen Dioxide
NOD	Nitrogen Oxide Derivates
O <sup>2-</sup>	Superoxide
O <sub>3</sub>	Ozone
PBS	Phosphate Buffered Saline
PEN	Penicillin
RNA	Ribonucleic Acid
ROS	Reactive Oxygen Species
RT	Room Temperature
SFM	Serum Free Medium
SLM	Standard Litres Per Minute
STREP	Streptomycin

## III. Table of Content

I. Summary .....	II
I. Zusammenfassung.....	II
II. Abbreviations .....	II
III. Table of Content.....	III
1. Introduction.....	1
1.1 Function and structure of human skin .....	1
1.2 Wound healing and the significant role of fibroblasts .....	4
1.3 Basics about plasma .....	7
1.4 Natural and artificial plasmas and its usage .....	9
1.5 CAP sources .....	12
1.6 The $\mu$ APPJ and difficulties in CAP research .....	14
1.7 Impact of CAP on cell culture media .....	15
1.7.1 Basics of NO and nitrogen species.....	15
1.7.2 Impact of NO and nitrogen species on wounds.....	18
1.7.3 Basics of hydrogen peroxide.....	19
1.7.4 Impact of hydrogen peroxide on wounds .....	20
1.8 Studies approach .....	22
2. Materials and methods .....	23
2.1 Materials .....	23
2.1.1 Cells .....	23
2.1.2 Common materials .....	23
2.1.3 Cell culture.....	24
2.1.4 Chemiluminescence detection (Nitrate, Nitrite) .....	25
2.1.5 Hydrogen peroxide and catalases control .....	25
2.1.6 Hydrogen peroxide photometry.....	26
2.1.7 Fluorescence photography .....	26
2.1.8 Operative equipment .....	26
2.1.9 Devices and equipment.....	27
2.1.10 Software .....	28
2.2 Methods .....	30
2.2.1 Cell culture.....	30
2.2.2 Cell subculturing.....	30
2.2.3 Cryopreservation .....	31
2.2.4 Cell isolation .....	32

## Table of Content

2.2.5 Plasma/CAP source and its characterization .....	33
2.2.6 Treatment methods.....	34
2.2.7 CellTiter- Blue® cell viability assay.....	35
2.2.8 Fluorescence microscopy .....	36
2.2.9 Measurement of hydrogen peroxide .....	36
2.2.10 Reductive gas-phase chemiluminescence .....	37
2.2.11 Nitric oxide and nitric dioxide Assay.....	38
2.2.12 pH-Value assay .....	39
2.2.13 Evaporation assay.....	39
2.2.14 Temperature assay .....	39
2.2.15 Dissolved oxygen assay .....	39
2.2.16 Statistical analysis.....	40
3. Results .....	41
3.1 Plasma characterization .....	41
3.2 Fluorescence microscopy of human dermal fibroblasts after helium gas treatment with the $\mu$ APPJ.....	42
3.3 Treatment of buffer with the $\mu$ APPJ.....	44
3.4 Treatment of human dermal fibroblasts in buffer with the $\mu$ APPJ .....	47
4. Discussion .....	53
4.1 Gas flow of plasma jets without enough buffer medium on cells leads to strong drying-off effects .....	53
4.2 Treatment with $\mu$ APPJ induces chemical/-physical modifications in buffer .....	53
4.3 Treatment with $\mu$ APPJ reduces cell viability .....	55
4.4 Chances of the $\mu$ APPJ in clinical usage for treatments of wounds and other tissues .....	57
4.5 Ambient atmosphere and system's gas tubing could affect the plasma characterization and biological effects.....	60
5. Conclusion .....	62
6. References.....	63
7. Acknowledgment.....	73
8. Supplement material.....	74
7.1 Material of gas delivery system affects OEC spectra and CAP-induced accumulation of hydrogen peroxide, nitrite and nitrate.....	74

# 1. Introduction

## 1.1 Function and structure of human skin

The skin is the largest and heaviest organ of the human being. Its total area amounts up to 1.6-2 m<sup>2</sup> and its thickness to 1.5-4 mm, neglecting the subcutis. Including the subcutis the thickness can reach up to several centimeters. The entire weight is about 3 to 20 kg. The areas of bodily orifices are transition zones of the outer skin to the mucous membrane of the inner surfaces of the body. Hence, these regions are predestinated to be involved in pathologic processes of the outer skin or could even be the origin of manifestations of diseases [1]. However, the derma fulfills different life-sustaining and psychosocial chores. It is the first protective barrier to active and passive pathogenic impacts and enables a boundary of the internal organs and tissues to the environment. In case of an injury it is possible that the organism loses large amounts of needed liquids, electrolytes and proteins that can cause respective metabolism disorders. Therefore, extensive skin diseases like toxic epidermal necrolysis, psoriasis-erythrodermia or most serious burns can lead to death [1]. Besides, the skin has crucial role in psychosocial communication, especially the face region. Due to its appearance one can draw conclusions about age, affects, spiritual condition treats or even internal diseases of one's opposite. Skin condition and look determine to a great extent the self-image. Therefore, visible, deforming scars or diseases aftermath can cause heavy psychological dilemmas. Accordingly both physiological and pathological state of the derma has a particular psychosocial dimension [1]. Referring to this fact the skins appearance of the patient should be implicitly maintained to avoid psychological trauma [1, 6].

After birth, human skin is frequently confronted with a variety of possible dangers. To the most important hazards are diverse impacts numbered, that start with coldness, heat, ionizing or nonionizing irradiation, desiccation and end with chemical substances, gems or allergens [6]. Physiological stimuli could strengthen and stabilize the functions of the derma, but if stimuli exceed a specific threshold they can become pathologic [1]. Moreover, a sensory function is given through various delicate tactile, heat, coldness or pain receptor cells. These

## Introduction

system serves also as an alarm feature to ensure the soundness of the derma [7]. Though this perception spectrum is limited – microbial noxes or specific irradiation noxes like ultraviolet radiation or ionizing emission cannot be directly noticed. Thus, these impacts only become conscious by skin damages due to this exposure [1].

However, to repel of viruses, bacteria or fungi an acidic biofilm is found on the derma with a pH-value of 5.5 consisting different anti-microbial proteins like defensins or lysozymes as a first line of defense. If germs penetrate the corneous, shielding surface, the skin can trigger an inflammation reaction as an organ of the immune system to encounter the threat [1, 6]. To encounter heavy temperature fluctuations of the ambient a reactive temperature regulation ensues due to controlled blood circulation in conspiracy with perspiratory glands. Up to 90 % of blood perfusion conduces thermoregulation, only 10 % nutrition [1]. Furthermore, the derma offers a highly efficient storage and metabolism mechanisms. The skin can save large amounts of liquid as edema or energy in form of fat. Different physiological and pathological metabolites can accumulate in the skin (e.g. porphyrins, amyloids) [1]. Besides, sebaceous glands nearby hair roots produce sebum to create a protective hydro lipid coat to prevent desiccation of topmost layers [6].

The derma itself is quite complex and composed of various components. It is not only a surface organ (also known as “Integument”) but also a layer organ involving three main stratum: uppermost the multilayered, keratinizing, self-renewing epidermis, following the high-fiber dermis and the subcutaneous fat tissue that both serves as high efficient isolation layer against temperature variations and mechanical pressure (see figure 1) [1, 6]. The non-vascular first layer, the epidermis, contains up to 90 % keratinocytes that convert to acaryote corneocytes through their way from the basal membrane to the surface. The morphologic-histologic manifestation of this process is the subdivision of the epidermis: direct above the basal membrane the stratum basale is found, where the stem cells provide constant renewal. Alongside the basement membrane, pigment providing melanocytes, immunologic dendritic cells (Langerhans-cells) and scattered sensory Merkel cells exist [1, 6]. Overhead the stratum spinosum is given. This multilayered area contains great polygonal keratinocytes that offer

## Introduction

peaked evaginations [6]. In the upper stratum granulosum are basophile keratohyalin granules located, that put out vital and necessary structure proteins to feed the stratum corneum. The uppermost stratum corneum is composed of the stressed acaryote corneocytes that serve as an important defense to mechanical pressure and chemical noxes. This whole differentiation process from

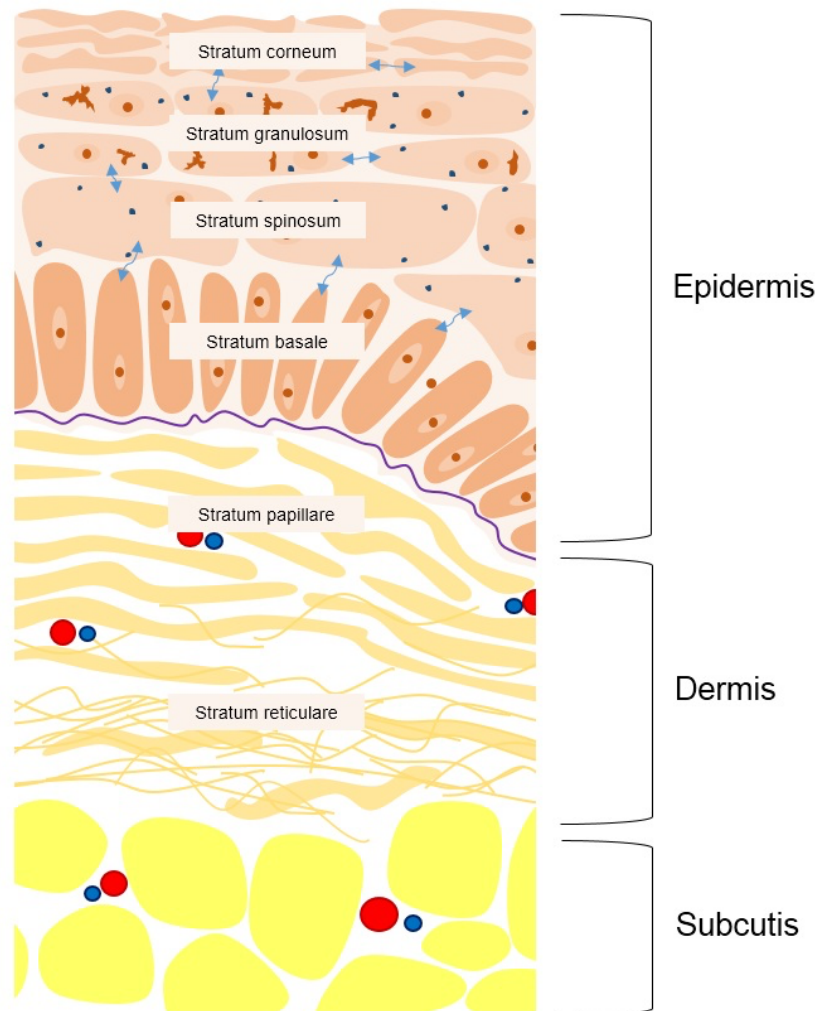


**Fig. 1 Layers of the human skin.** The topmost epidermis consists to 90 % of keratinocytes that change to corneocytes [1]. This metamorphosis is shown in the different layers of epidermis: starting the differentiation at the stratum basale and subsequently ending at the stratum corneum. Amongst epidermis and the fat-rich subcutis the strong vascularized dermis is found, districted in stratum papillare and reticulare that is rich in collagen (own illustration based on [6]).

keratinocyte to corneocytes takes up to 6 weeks [1, 6]. Underneath the fibro-elastic dermis is situated. This layer offers the conjunction tissue intermediate the epidermis and the subcutaneous fat tissue beneath. It principally consists of autochthonous connective tissue cells, the fibroblasts, that have a significant role in the healing process of wounds and neoformation of tissue, and extracellular matrix made of collagen fibers and basic substance. However, it is divided into a strong vascularized stratum papillare and a collagen-rich stratum reticulare and provides both various mobile inflammation and immune cells (e.g. macrophages,

mast cells and lymphocytes). Due to its characteristics, the dermis provides the skin its particular tearing strength and elasticity. The third under most layer, the subcutis, generally consists of adipocytes and connective tissue [1, 6-8].

### 1.2 Wound healing and the significant role of fibroblasts

A wound is a dissociation of tissues accompanied by local vascular insufficiencies, possible contaminations and a various pronounced loss of substance. Principally a distinction is made between lesions with lower and higher-level injuries that influence diagnostic and therapy. Parameters of particular importance are widening and deepness, collateral sores, location and feasible pre-injuries [4]. Besides, a vital determination is made between mechanical, thermic, chemical, actinic or chronic wounds [5]. The consequential group of mechanical wounds distinguish in open wounds (lat. *Vulnus*; the skin is served), closed wounds (lat. *Laesio*; skin and mucosa is intact), avulsions or décollements and amputation traumas [4].

Disregarding chronic wounds, the human body is able to close emerged tissue defects. In general two pathologic regenerations are given: the complete regeneration that depicts that the lesion gets substituted by functional equivalent cells and the physiological state is reintegrated, and the uncompleted regeneration in which the sore heals under forming a functional inferior tissue (scar tissue) [5]. The process of wound healing is segmented in three main phases (see figure II). The first phase, the substrate phase, lasts approximately for four days and is characterized by hemostasis and inflammation litigations. Directly after injury blood and blood plasma pour into the wound gap. Besides of purging the sore the contact of thrombocytes and collagen triggers the blood clotting and the gap gets filled with dense fiber clusters. Activated macrophages phagocytize necrotic tissue and release nitrogen monoxide and oxygen radicals and other mediators to ensure an anti-microbial milieu and to attract other immune cells [5]. Subsequently, the proliferation phase sets in. This phase lasts for up to two weeks and is specially marked by forming granulation tissue. Fibroblasts gain crucial importance during this time frame since they are indispensable needed for this process. The word “fibroblast” designates all

## Introduction

stroma cells that not express more specific markers which lead to a defined mesenchymal cell line. Hence, the characteristics of fibroblasts differ between tissues and organs and appear very heterogeneous. Even in the dermis itself different subtypes of fibroblasts are found [9-13]. These long-living cells produce the extracellular matrix (ECM) and control its composition that is crucial for the healing wound [14]. Matricellular proteins, glycosaminoglycans, proteoglycans as well as fibrin, fibronectin and collagens include these products [9, 15]. The most potent fiber-forming protein is collagen. Collagenous clusters are responsible for the structural tearing strength of the wound and facilitate migration, chemotaxis and cell adhesion what is indispensable for a proper healing. Conversely, a too high density of these interwoven fibers lends among other factors to hypertrophic scarring in further wound healing processes [15-19]. These collagen fibers can be subdivided into fibrillar (Type I-III, V) and nonfibrillar (Type IV, VI-VIII, XIV) groups that are integrated in the wound healing process and are essential for the fibroblasts function [9]. However, the ECM has an effect of the fibroblasts itself. Different gene expressions are influenced by the laxity or rigidity of the ECM, e.g. apoptosis, the matrix metalloproteinase activity or the differentiation into myofibroblasts. Hence, a sophisticated interaction between fibroblast and ECM is given [20-26]. During the proliferation phase capillaries grow from the edges into to wound gap forming a dense web between the active fibroblasts and ECM. Thus, a strong vascularized, young conjunctive tissue fills the sore and seals the yawning wound. Macroscopically, the tissue appears very pithy, accordingly causing its name "granulation tissue" [5]. In the following differentiation phase starting in the third week the ratio of ECM exceeds the number of fibroblasts vigorously. Meanwhile the quantity of conjunctive tissue cells decreases and a cell-poor but fiber-rich scar tissue forms in the central wound region. The scarring is susceptibly influenced by the dynamic equilibrium of collagen enrichment and degrading. Through wound contraction, another vital function of fibroblasts, that are modified to myofibroblasts due to the ECM and other various factors, the wound area decreases up to 50-99 % of the origin defect region. However, with epithelialization due to peripheral epithelial cells the wound healing finishes. Subsequently a reddish, slight elevated compared to ambient skin scar remains, that adjusts to skin level and pales during the following weeks [5, 9].

## Introduction

Wounds and tissue defects heal depending on genesis, kind and treatment of the sore. These regularities influence a suitable therapy. Four different types of wound healing are given. The primary wound healing can be observed if the wound edges are even, front each other without tension, no essential vascular issues are given and the sore is not contaminated, e.g. after a surgical procedure. Granulation tissue is just slightly produced and the edges merge rapidly causing an approximately invisible scar. Secondary wound healing happens if the wound edges diverge wildly, a vital disturbance of blood supply occurred, or a high level of contamination is given. Wound closure follows due to producing much granulation tissue, contraction of myofibroblasts and epithelialization. Result is an often broad, long, cosmetically not appealing scar that also could cause functional issues. The third kind, the regenerative wound healing happen when just superficial defects of epidermis or mucosa occur. The wound heals completely with an entire recovery of function and appearance of the skin. Similarly, one can observe the same healing under scab, whereas here the

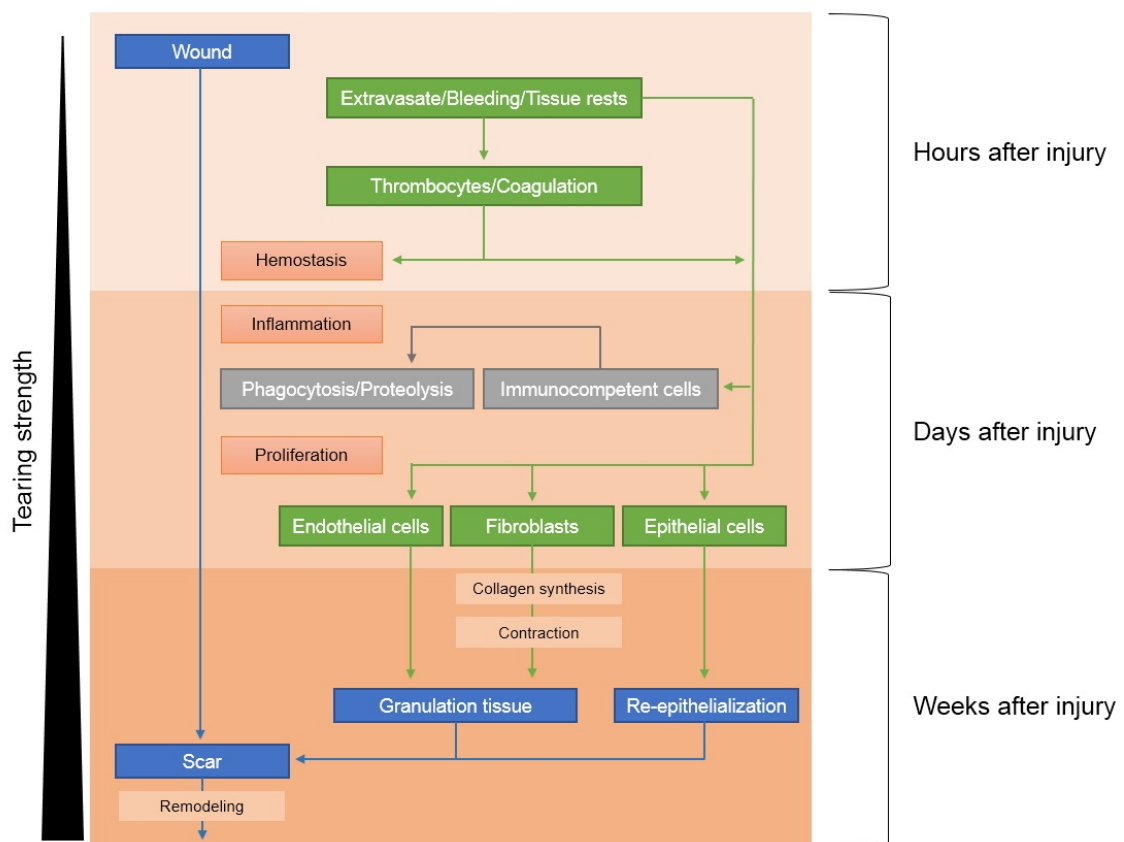


**Fig. II Phases of wound healing featuring the prominent role of fibroblasts.** Hours after receiving a lesion the mechanisms of inflammation and hemostasis take a significant part that outreaches into days. The days and weeks afterwards are characterized by granulation tissue that is produced by fibroblast which migrate the wound gap. Subsequently the amount of original tissue cells decrease and is replaced by collagen-rich tissue – the scar (own illustration based on [4, 5]).

danger of secretion congestion and therefore healing issues exist. As opposed to this process, the fourth, reparational wound healing includes desmoid scar tissue to bridge the skin defect. Thus, this healing form involves the primary and secondary wound healing [4, 5].

### 1.3 Basics about plasma

The term “plasma” is not just, as usually known, a description for the liquid, cell-free part of blood, but also describes a special, stimulated state of aggregation in physical science, well-established as the fourth state of matter. Sir William Crookes described in 1879 what we know today as plasma, in 1929 Dr. Irving Langmuir first used the term “plasma” to name the ionized gas [27].

Through the input of energy, it is possible to transfer a solid matter to a liquid and further to a gas – which is associated with an enhancement of the movement of the atoms and molecules (thermal energy) and less interparticle binding forces in a substance. Thus, the state of a matter depends on its thermal energy and the interparticle binding force. The state of completely free mobility is reached in the gaseous state of a substance. If one pushes the gaseous state more forward and induces enough energy in term of warmth or strong electric fields the thermal energy of particles overcome the binding force. That leads to that the molecules dissociate, and the outermost electrons will be stripped away. A partly or

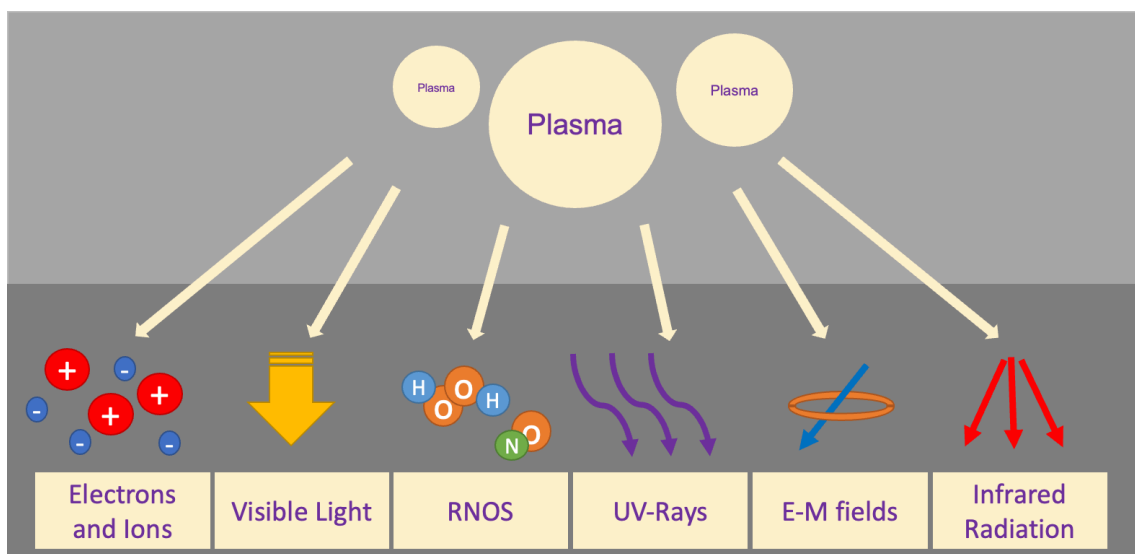


**Fig. III Efficacious components of physical plasma.** Different agents are emitted – electrons/ions, visible light, RNOS, UV-Rays, electromagnetic fields (E-M fields), infrared radiation (Own illustration based on [2]).

## Introduction

completely ionization of the particles results. Free electrons and positive charged ions in an overall neutral gas with a higher reactivity is the consequence – a phase transition has occurred. These plasmas emit electrons and positive charged particles, electromagnetic radiation, UV-Rays, infrared radiation, visible light and produce reactive oxygen and nitrogen species (See figure III). Furthermore, physical plasmas are electric conducting due to its ionization. The quantity and quality of its properties depends on different parameters, such as feeding gas mixture (i.e. argon, helium, ambient air), the stream of uncharged and charged particles (negative and positive ions as well as electrons and atoms), molecules (OH, NO, O<sub>3</sub>, H<sub>2</sub>O<sub>2</sub>, species etc.), input energy and environment pressure [2, 28, 29]. Naturally, a low number of ionized atoms can be found in every gas, due to high-energy radiation or collisions with fast particles. But only if the number of ionized atoms and electrons reaches a significant percentage of a gas, one can determine a substance as a plasma. Hence, to estimate the ionization grade of a gas the Saha ionization equation is used that describes the reaction equilibrium between ionization and recombination processes (see figure IV) [2, 30, 31].

$$\frac{n_i}{n_n} \approx 3 \times 10^{27} \frac{T^{3/2}}{n_i} e^{-W_{ion}/T},$$

**Fig. IV Saha ionization equation to determine the part of ionized atoms of a matter.** The equation describes the equilibrium of ionization and recombination processes.  $T$  = Temperature,  $W_{ion}$  = Ionization energy of neutral particles (eV),  $n$  = Density ( $1/m^3$ )

The temperature naturally increases by phase transitions from solid over liquid and gaseous to plasma, depending on the thermal motions of electrons, atoms and ions. Due to collisions between heavy particles and hot electrons in a high density in a common physical plasma at atmospheric pressure, almost all particles approach thermal equilibrium. That means, all particles, regardless if electron or heavy particle, have the same temperature. According to that, the temperature reaches over several thousand degrees due to the high density of hot electrons and makes it impossible for direct treatments on human skin or wounds [32]. Hence, this class of plasma shall be named *thermal plasma*. However, if the atmospheric pressure plasma discharge is fast enough, it can result in a state of thermal non-equilibrium in which the temperatures of a plasma oscillates between 25 °C up to 45 °C. In this case of fast discharge, the plasma is just slightly ionized, and the particles are able to cool down and reach room

temperature. Regarding to this, due to the huge mass difference between the static, heavy particles with low temperature and the fast moving, hot electrons, the plasma temperature is set by the heavy particles. This class of plasma is usable as a treatment opportunity to human skin and shall be named *cold atmospheric plasma* (CAP) [29, 33, 34]. Subsequently, a distinction can be drawn – between *thermal* and *non-thermal plasma* (CAP). Regarding on pressure and feeding power, thermal plasma or CAP is generated. Moreover, the density and the pulse of the feeding power influences if the plasma approaches the thermal equilibrium state. The higher the pressure, the more collisions happen and the temperature of the plasma increases. The feeding power for CAP are mostly local overloaded electric fields [32].

### 1.4 Natural and artificial plasmas and its usage

In general, another distinction can be drawn between natural and artificial generated plasmas. Natural plasmas appear in terms of lightnings, solar storms, aurora borealis and up to 99 % of the visible matter of the whole universe. Because of its special reactivity artificial plasma treatments are ubiquitous, even though it is not present in our common awareness, whether in experiments of nuclear fusion technology to solve the energy issues of humanity, the light in neon tubes and energy saving lamps, industrial welding with hot thermal plasma or the creation of moving pictures in our plasma TVs. It is even used for treatment of surfaces of credit cards, plastic bags, materials of cars and other vehicles, the plasma is mandatory in the industry [2].

Against this background a connection to a medical treatment is hard to imagine. The biochemical usage of physical plasma can be split into three main aspects, that are difficult to separate. The first is the already named surface modification, that is also used for biological relevant surfaces to improve the biological compatibility or functionality of medical products as e.g. implants or liquids for cell cultivation [35]. However, studies show that plasma treatment of implants can change the free energy of surfaces and therefore have significant effect of e.g. collagen adhesion [36].

## Introduction

The second intensively researched field of application is the inactivating and eliminating of microorganisms. In 1996 it was reported for the first time, that it is possible to kill bacteria with plasma [37]. The plasma treatment represents a high-effective alternative to the established sterilisation and disinfection methods, because neither high temperature, radioactive radiation nor toxic chemicals, that are not applicable to a number of medical and hygienic materials, are necessary. How this mechanism of eliminating microorganisms work is not completely explained – drawn to actual state of knowledge it is possible that physical mechanisms (free radicals, UV-Rays, reactive species) as well than biological mechanisms (such as cell membrane and DNA damages) are responsible for inactivating bacteria [29, 38]. Numerous studies with varying parameters prove the efficacy of CAP against gram negative and positive bacteria, biofilm producing bacteria, spores, viruses und fungus [39-46]. It could even be shown that plasma treated distilled water (5 min treatment with CAP fed by ambient air) has an antimicrobial impact on various germs [47]. Moreover, is already known that plasma not just inactivates and kills the microorganisms, but also removes organic material and biofilms completely, such as on catheters, medicals implants or teeth [2, 48]. This is a matter of interest, since infection transmitting proteins e.g. prions, that are not assailable with conventional methods, become more important in the last years. Indeed, the proof, that the infectivity of prions is efficient reduced by CAP treatment has still to be done, but its reduction is already shown in prion protein models [49]. Additionally, no resistances of microorganisms against physical plasma are known [50, 51]. These two methods of plasma application can also be referred as indirect treatments, since the wound is not directly treated.

The third, direct medical treatment with plasma is usually used e.g. in term of blood coagulation, cosmetic applications, wound healing and bacterial triggered dermatoses. The local application of thermal plasma for blood coagulation and obliteration of angiodysplasia and removal of tumors happen since ca. 30 years. The device of choice is often the Argon plasma coagulator (APC) in many surgical fields. The effect based on thermal issues and impacts the protein denaturation and desiccation of tissue [52-54].

## Introduction

Referring to cancer treatment, through the controlled induced apoptosis or necrotic cell death tumor cells could be effectively method of fighting cancer, regardless to operated plasma source, since many different sources were used in these studies [55-62]. For instance, Arndt, Wacker [55] demonstrated an irreversible cell inactivation of melanoma cells after a 2 min treatment with a hand-held CAP source (Surface Micro Discharge and therefore a hybrid source).

The US Food and Drug Administration allowed the so-called plasma skin regeneration technology (PSR) for wrinkle smoothing and skin rejuvenation in 2005. Therefore, a hot, but fast cooling plasma is used. The application is carried out by a plasma source fed by a nitrogen gas. The treatment triggers collagen production, a reconstruction of the dermal architecture due to controlled thermal damages and inhibits the generation elastic fibers, that could be histological confirmed [29, 63-65]. Besides wrinkle treatment this method is suitable for actinic keratosis, seborrheic keratosis, virus papilloma, scars and light damaged skin or in combination with aesthetic surgical operations. During the treatment, local or systemic analgesics are necessary. Various studies confirm the benefit of this application with a wrinkle reduction of up to 50 % [66]. However, it becomes apparent that through oxidative species (in this case: H<sub>2</sub>O<sub>2</sub>) an improvement of tooth bleaching is shown, so that the plasma treatment is also interesting for the dental application [67, 68].

Positive impacts on wound healing processes are mostly attributed to the disinfecting influence of plasma. Since 1970 it is known that more than 10<sup>5</sup> colony creating units per gram of tissue of  $\beta$ -hemolytic streptococcus, staphylococcus aureus and pseudomonas aeruginosa is enough to interfere with the process of wound healing [29, 69]. The healing process is also inhibited if more than four different bacteria species are found in a wound [70-72]. Besides this, studies proved that conducive to healing processes is the exogenous generated NO by plasma [73, 74].

## 1.5 CAP sources

Cold atmospheric plasmas sources can be distinguished into three CAP technologies (see table I): the direct, indirect and the hybrid kind.

- 1 In case of direct plasma, the tissue or a surface, i.e. the skin, functions as an electric electrode and enables that electricity can stream through the body [75]. For this purpose, the typical source is the *dielectric barrier discharge* device (DBD) [76]. This kind of discharge is called 'barred', because the electrodes are divided by a non-conducting layer (the barrier). These discharges do not occur massive and potentially catastrophic like lightnings, but instead much softer in term of many small micro discharges of ca. 100 ns duration from barrier to counter electrode. A near homogeny 'curtain' of discharges is normally given – presupposed the gaps from barrier to counter electrode are exactly even, mostly amounts 1 mm.
- 2 The indirect plasma is generated between 2 electrodes and is ejected to the destination area as an effluent [39, 77, 78]. Hence no barrier is given, the individual discharges can be much stronger, the transport of particles and generated molecules is carried out by gas flow and diffusion. Most devices produce thin *plasma jets* with just a few millimetres' diameter. Greater areas are treatable if many of these jets are merged or respectively treated by multi electrode systems simultaneously, a great advantage to direct sources. Another benefit is that the interspace between discharge and tissue is variable, given that the skin is not in need as a counter electrode following a much easier treatment of patients.
- 3 The hybrid plasma, also known as 'barrier coronal discharges', link the named technologies. The plasma is generated like a direct plasma, but because of a grounded electrode net no electricity flows through the tissue [79]. In contrast to DBD devices there is no air gap between barrier and counter electrode in which micro discharges could happen. However, the counter electrode must be structured (i.e. a net). These stressed micro-discharges act parallel to the surface of the dielectric barrier, therefore these electrodes were called *surface micro discharge* (SMD). These SMD systems

are completely autonomous to space between tissue and the plasma device [29].

	<b>Direct Plasma</b>	<b>Indirect Plasma</b>	<b>Hybrid Plasma</b>
<b>Device</b>	Dielectric barrier Discharge	Plasma Jet	Barrier coronal discharge
<b>Generating and Characterization</b>	Tissue as counter electrode, electricity flows through body	Produced between two electrodes above target tissue	Combination of both technologies - no electricity flows through body
<b>Feeding Gas</b>	Air	Noble Gas/ air	Air
<b>Interspace between device and target</b>	mm	mm -cm	mm
<b>Reactive Species</b>	Produced mainly in plasma	Produced due mixture of plasma and air	Produced mainly in plasma
<b>UV Radiation</b>	low	high	low
<b>Gas Temperature</b>	Room temperature	Mainly room temperature	Room temperature
<b>Plasma Density at target</b>	High	Low	High

*Table 1 Characterization of different CAP sources. One can differ between direct, indirect and hybrid plasmas that have all diverse attributes based on [29].*

Most CAPs are fed with helium or argon feeding gas, but ambient air or other mixtures are used as well. A magnificent advantage of CAPs is the possibility to design a plasma to gain the requested composition and effect (chemical cocktail), depending on the circumstances while generating (feeding gas, electricity, electrodes, pressure, etc.) [28]. No general admitted designations attributed to the consistence of plasma are given. Threshold values exist just relating to electricity, UV radiation (maximal allowed dose 30  $\mu\text{W}/\text{cm}^2$  (see SCCP European Commission Report 0949/05) and the generation of reactive species (threshold value for ozone 50 ppb see CPSC Consumer Products Safety Commission –

Report from 06/09/26, for NO<sub>2</sub> 2 or 5 ppm and 25 ppm for NO over a duration of 8 s, see US National Institute for Occupational Safety and Health NIOH) [29, 38].

Obviously most important is the safety of a patients during treatments. Therefore, it is essential to check potential risk factors as electricity, thermal damage to tissue and skin, the amount of UV radiation, the treatment length and the gas mixture. Thus, Lademann *et al.* [80] could show through examinations of pig ears and adhesive tape tearing tests of voluntary probands, that after a treatment of an argon gas fed plasma jet lesser than 1 % UV light reaches living skin cells, because every single of the 15 to 25 corneocytes layer of the human skin absorbs ca. 25 % of radiation. Even the temperature impact was negligible.

### 1.6 The $\mu$ APPJ and difficulties in CAP research

A promising approach to ignite and keep plasma in a stable and cold state at atmospheric pressure is the spatially confining of CAP to a reduced dimension of 1 mm or less. These kinds of plasma discharges are often contemplated as *microplasmas* – a subdivision of plasma, which include high concentration of radicals [81-83]. The device that we used is a microplasma-producing jet ( $\mu$ APPJ) and belongs to the indirect plasma sources. Regarding the European COST (European Cooperation in Science and Technology) Action MP 1011, the micro-scaled  $\mu$ APPJ developed by Schulz-von der Gathen and co-workers was selected for this study – the COST reference microplasma jet.

$\mu$ APPJs can be operated with helium feeding gas and have been studied in various research groups for its clinical use [84-93]. In this connection, the difficulty nowadays is that in these numerous investigations all over the world self-made CAP jets were used as research objects [94-97], what makes it nearly impossible to compare the gained results. This results in impairment to further research and delays the understanding of cold atmospheric pressure plasma and its interaction with human cells and tissue [98], following a deferred everyday medical usage [99].

Besides the already referred positive effects of CAP, studies proved that various kinds of CAP can induce cell death in different mammalian cell such as

endothelial cells, lymphocytes and keratinocytes. This can represent a major setback in clinical treatment for wounds or inflammatory skin diseases [92, 100-105]. However, the vitality of cells depends on its direct environment. This contains a stable osmolality, pH, temperature and a sufficient quantity of oxygen and nutrient. In this regard, plasma jets can dry-off *in vitro* as well as *in vivo* the cells surroundings, especially when high gas flows are used (up to 6 slm). This treatment limits the application time of a CAP due to cell death because of desiccation. The  $\mu$ APPJ in this study can be operated with a gas flow range of 0.25 – 1.4 slm, preventing these drying-off effects which allows longer treatment times.

## 1.7 Impact of CAP on cell culture media

Cold atmospheric plasma has various effects on cell culture media (NaCl, PBS), such as acidification [106], enrichment with nitrite and nitrate concentrations [58, 62, 107, 108] and generation of hydrogen peroxide [108, 109]. Through the increase of NO and H<sub>2</sub>O<sub>2</sub> the microenvironment of cells could be susceptibly affected, causing an enhanced or impaired viability of human dermal fibroblasts (HDFs). Therefore, the crucial role of nitrogen species and hydrogen peroxide in human cells shall be explained in the following chapter.

### 1.7.1 Basics of NO and nitrogen species

The free radical nitrogen monoxide (NO) is an inorganic gas, that is dissoluble in liquids up to a concentration of 2 mM. Due to its small dimension and its lipophilia it can diffuse through biological membranes [110]. As a radical its reactivity is very slight because of its short half-life of a couple of seconds [111,

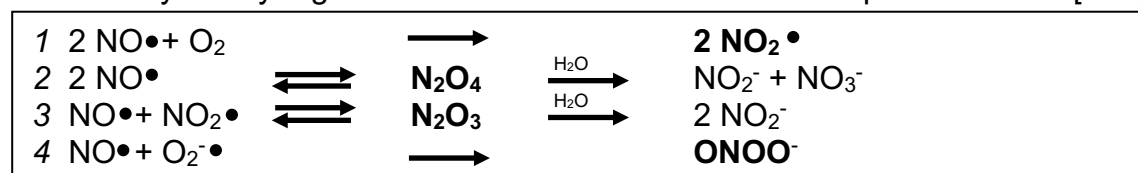


**Table II Reaction equilibrium of NO with O<sub>2</sub> in a Solution.** Stable end products are Nitrite (NO<sub>2</sub><sup>-</sup>) and Nitrate (NO<sub>3</sub><sup>-</sup>). Instable, reactive intermediate products (species) are fat marked (N<sub>2</sub>O<sub>4</sub>, N<sub>2</sub>O<sub>3</sub>, ONOO<sup>-</sup> and NO<sub>2</sub>) (based on [3])

## Introduction

112]. NO reacts *in vivo* as also *in vitro* with oxygen through higher nitric oxides ( $N_2O_3$  and  $N_2O_4$ ) to the stable end products nitrite ( $NO_2^-$ ) and nitrate ( $NO_3^-$ ) (see table II).

In this process, high reactive and instable intermediate products accrued – the *reactive nitrogen species* (RNS), which can interact with a broader spectrum of biomolecules than NO alone [113]. NO is generated enzymatically and non-enzymatically in the human body. Nitrogen monoxide synthases are responsible for the enzymatic biosynthesis of NO in cells. These synthases can be subdivided into three isoforms (nNOS, ecNOS and iNOS) with a huge structural resemblance and identical catalytic mechanisms [114], that catalyse the 5-electron-oxidation of L-Arginine and molecular oxygen to NO and L-Citrulline. Relevant cofactors for the NO-synthesis are NADPH, FAD, FMN, calmodulin,  $BH_4$  and protoporphyrin IX [115-118].

The first two isoforms nNOS [118] (first found on neuronal cells) and ecNOS (first found on endothelial cells) are regulated by enzyme activity, in which the  $Ca^{2+}$ -concentration has a critical role [119]. An increase stabilizes the calmodulin conduction on the enzyme's binding site and induces therefore the NO-synthesis [120]. The third isoform is not physiological expressed, but typically due to inflammation or immunogen stimuli (IFN- $\gamma$ , TNF- $\alpha$ , IL-1 $\beta$ ) or bacterial parts (LPS) induced [121]. Therefore, this NOS is called induced NOS (iNOS). Although calmodulin is necessary for NO-synthesis, the enzyme activity is not influenced by  $Ca^+$ -concentration changes [122, 123]. In comparison to NO-concentrations at pico molar range generated by eNOS and nNOS the NO-concentration produced by iNOS can reach easily micro molar amounts [124].

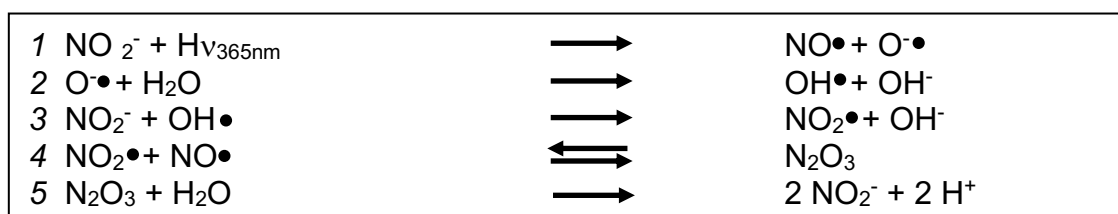


**Table III Radiation induces diversion of nitrite anions.** In equilibrium 4 is demonstrated, that the generated NO is partly consumed, therefore the free available number of NO is reduced.

Non-enzymatically NO can accrue as a sequence of photolysis and pH-induced destruction of nitrite anions ( $NO_2^-$ ) (see table III) [125]. In the first case the nitrite anions in a nitrite containing solution are divided due to electromagnetic radiation

## Introduction

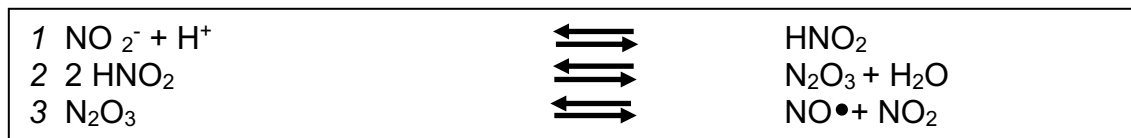


**Table IV Diversion of Nitrite under acetous conditions.**  $\text{HNO}_2$  is in an equilibrium with  $\text{N}_2\text{O}_3$ , that can dissociate spontaneously to  $\text{NO}$  and  $\text{NO}_2$ .

at UVA-Range (354-355 nm) and subsequently  $\text{NO}$  and oxygen anions ( $\text{O}^-$ ) are generated. At acetous conditions the nitrite anions in liquid solutions are in an equilibrium with its conjugated acid  $\text{HNO}_2$  (see table IV).  $\text{HNO}_2$  in turn is in an equilibrium with  $\text{N}_2\text{O}_3$ , that can divide spontaneously to  $\text{NO}$  and  $\text{NO}_2$ . Whereas spontaneous division at physiological pH is very rare, under acetous conditions are more often. Although, the photolysis of nitrate is described and offers another biological source of  $\text{NO}$  [126].

$\text{NO}$  itself is biological signal and effector molecule that exhibits physiological and pathological properties. It features as an effective cellular toxin a capacity in the unspecific immune reaction, in which it protects the organism against pathogens [127] and tumor cells [128]. However, it takes also part in destroying body's own cells and tissues [129], enhanced inflammation processes [130, 131] and can also be responsible for different skin diseases, e.g. psoriasis, skin tumors and impaired wound healing [132-135].

$\text{NO}$  interacts in that case with nucleic acids and leads to a  $\text{NO}$ -related DNA-deamination and string breaks [136]. High  $\text{NO}$  concentrations can conduct apoptotic or necrotic cell death due to damages of DNA and impairments of energy metabolism, calcium hemostasis and mitochondrial function [137, 138]. In line with unspecific immune reaction generated  $\text{NO}$  and RNS (especially  $\text{ONNO}^-$ ) serve as cytotoxic molecules against invading microbes [139]. Moreover,  $\text{NO}$  and its intermediate and reaction products lead to protein modification and destruction of metal-sulfur-cluster and zinc finger motives in different cytosolic and membranous proteins (Channels, signal proteins, transcription factors and enzymes). This in turn causes modification of enzyme activity [140] or indirect mediated changes in expression of genes [141].

In general, the specific biological efficacy of  $\text{NO}$  depends on participating cells and cell systems as well as the time of effectiveness and local concentration generated by enzymatic and non-enzymatic  $\text{NO}$ -production. Therefore,  $\text{NO}$  produced by eNOS leads to a relaxation of plain muscle cells *in vivo* and has a

crucial role in regulating the vascular tonus [120, 142]. In addition, NO generated by nNOS takes part as a significant neurotransmitter in the peripheral and central nerve system [117].

Besides the toxic and regulating properties of NO studies evidence that high NO-concentrations can communicate a potent protection against cell damages and therefore prohibit an apoptotic or necrotic cell death. Hence, NO officiates as an antioxidant and protects the cell against ROS conducted lipid peroxidation [143, 144]. Accordingly, through the delivery of NO and activation of NO-related pathways the cell could be sensibly affected, since various processes of the human skin physiology are associated with NO [125, 145, 146].

### 1.7.2 Impact of NO and nitrogen species on wounds

As said NO controls the transcription numerous genes and is an important regulator of gene expression. This includes stress-protection-genes which code for heat-shock-proteins, chaperones and hemoxygenase-1. Besides, genes are controlled that are responsible for coding for regulation mediators of inflammation reactions (e.g. IL-4), reparatory enzymes (e.g. matrix-metal-proteinases) or growth factors (e.g. VEGF). These gene expression regulating abilities as well as the influence of regulation on cell mobility of fibroblasts, keratinocytes, monocytes and macrophages make NO to a key molecule in controlling wound healing and tissue regeneration [145]. This gains particular importance at iNOS-deficient mice, whose wound healing processes are significant delayed. In the first 72 h in the process of wound healing the activated iNOS produces high concentrations of NO that induces vasodilatation and functions antimicrobial [147]. The NO is accounted for an enhancement of proliferation of keratinocytes and fibroblasts. Hence, it plays a key role in reepithelialisation and is essential for the angiogenesis [148, 149]. Furthermore, it strengthens the collagen synthesis and leads to a hastening of wound healing. Thus, the application of NO-donors could increase the fibroblast's produces collagen amount in a wound [150, 151]. Besides, treatment of mice with nitrite containing ointment as a NO-donor-system led to a significant improvement of wound healing. However, S-nitrosated thiols

## Introduction

are already used in topic treatment on human skin and are used as antimicrobial and reepithelialisation supporting substances [152].

All these results underline the key role of enzymatic and non-enzymatic generated NO in wound healing, hemostasis and cell protection of skin [145, 153, 154].

### 1.7.3 Basics of hydrogen peroxide

Hydrogen peroxide, as a non-radical 2-electron reduction product of oxygen, has a crucial role as a signaling messenger in human cells. It gains particular importance in host defense and oxidative biosynthetic reactions [155, 156].  $H_2O_2$  is generated as product of different enzymatic reactions in peroxisomes, mitochondria and other cell parts or as a byproduct of aerobic respiration under basic conditions due to its high reactivity to other antioxidant systems [157-159].

The cellular generation and consumption of  $H_2O_2$  is balanced under steady state conditions. The main sources of  $H_2O_2$  production are superoxide dismutates (see table V) [160], the acyl-coenzyme A oxidases in peroxisomes and the flavin-

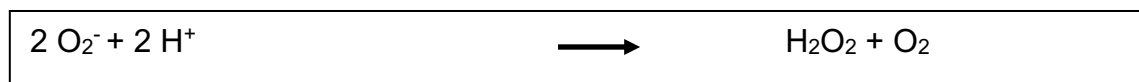


**Table V  $H_2O_2$  generation through superoxide dismutase.** *Superoxide dismutase reacts superoxide anion radicals and hydrogen to hydrogen peroxide and oxygen.*

dependent oxidases [161]. Most of these enzymes induce the dismutation of superoxide anion radicals, that are predominantly generated by mitochondrial electron transport chain and membrane-associated NADPH oxidases [162-164]. These NADPH oxidases are highly controlled by growth factors and cytokines [165]. However, macrophages and activated monocytes release superoxide [166], whereas neutrophils and eosinophils use oxidants as a disinfecting defense, also known as oxidative burst. In note, its shown that HDFs treated with intereleukin-1 or tumor necrosis factor-alpha release a significant amount of

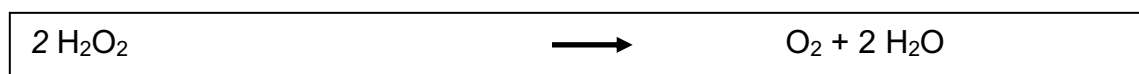


**Table VI  $H_2O_2$  reduction through catalase.** *Catalase dismutates hydrogen peroxide to oxygen and dihydrogen monoxide.*

superoxide resulting in  $H_2O_2$  related signaling, that gains a significant importance in managing wound healing and inflammation process [167]. The other main source is the respiratory chain-linked  $H_2O_2$  generation, that is mainly related to superoxide dismutase and the mitochondrial superoxide production due to cytochrome *bx1*-complex, also known as Complex III [168-170]. Mitochondrial Complex I and II are also described as independent sources of reactive oxygen species [171].

However, the amount of  $H_2O_2$  is under the fine control of scavenging enzymes such as glutathione peroxidase, peroxiredoxins and catalases (see table VI) [163, 164]. Catalase is predominantly located in peroxisomes, whereas glutathione peroxidase and peroxiredoxins are found in subcellular compartments [172, 173]. The metabolic sinks of  $H_2O_2$  are mainly related to catalytic and several peroxidic reactions underwent by catalase and diverse peroxidases. In addition to that, the concentration of  $H_2O_2$  depends on the diffusion away from its source, eventually across the membranes the extracellular space and other cells [174].

The main messenger attribute of  $H_2O_2$  includes its ability to oxidize diverse proteins with a particular specificity, highly depending on the reaction with nucleophilic cysteine thiolate groups [175]. This oxidation may cause the formation of unstable sulfonic acid, that also can be reduced again and react with other thiol groups to form disulfide bonds or hyperoxidate to react to sulfinic and then sulfonic acids [164, 176, 177]. These formations can lead to significant conformational changes resulting in different macromolecular interactions, functions, stability, activity and protein localization [178, 179].

### 1.7.4 Impact of hydrogen peroxide on wounds

In case of an injury of the skin, the amount of hydrogen peroxide accelerates in the microenvironment of the wound, reaches a peak and fades away. This specific dynamic is crucial for diverse functions, as such as dealing as an signaling molecule, disinfection of the wound and as a second messenger that catalyze reactions in other cells. The effects of hydrogen peroxide depends on the specific dose in the microenvironment. High concentrations lead to

## Introduction

proinflammation and oxidization to sterilize wound tissue, whereas low concentrations help wound healing as an important factor in promoting secretion of cytokines and removing debris [180]. However,  $H_2O_2$  also effects gene expression through different ways [181].

It is shown on an experiment on zebrafish, if the skin is injured, a rise in hydrogen peroxide amounts was detected in the microenvironment of the wound. This lead to an accumulation of leukocytes that peaked after 20 min and decreased again, highlighting the function of  $H_2O_2$  as an inflammatory initiator and a chemotactic signal [182]. The accumulation of the  $H_2O_2$  in wounds mainly depends on nicotinamide adenine dinucleotide phosphate (NADPH) oxidase [180], expressed on the plasma and subcellular membranes (especially of the mitochondria and the endoplasmic reticulum membrane) [183, 184]. Besides mechanical impairment of the wound, pathogen attacks and inflammatory cytokines lead to an activation of NADPH. NADPH oxidase convert one oxygen molecule in superoxide anion that transforms into  $H_2O_2$  due to superoxide dismutase [185].

Depending on which phase of wound healing happen,  $H_2O_2$  plays different roles in wound healing. During hemostasis stage  $H_2O_2$  triggers the cell surface tissue factor and therefore platelet aggregation. In Inflammation stage  $H_2O_2$  causes higher concentrations of leucocytes and cytokine secretion as a proinflammatory reaction as well as antioxidant gene expression as an anti-inflammatory reaction. In the cell proliferation and tissue remodeling stage the concentrations of vascular endothelial growth factor, cyclooxygenase-2 and epidermal growth factor receptor accumulate partly related to  $H_2O_2$  resulting in improved angiogenesis and therefore tissue formation and wound healing [186-191].

Furthermore, studies showed that hydrogen peroxide interfere with the balance of matrix metalloproteinases and tissue inhibitors of matrix metalloproteinases, resulting in high concentrations of  $H_2O_2$  lead to an increased impression of transforming growth factor (TGF)-1 and enhanced proliferation of fibroblasts [192].

It should be noted that it is crucial for wound healing to get the correct concentration of  $H_2O_2$  to an appropriate level to support wound healing and to avoid oxidative damages [193]. Just a few studies deal with  $H_2O_2$  effects on

## Introduction

chronic wounds, indicating the seen effects are mainly based on acute wound models.

### 1.8 Studies approach

The approach of this study was first to determine *in vitro* the impact of  $\mu$ APPJ treatment on the microenvironment of human dermal fibroblasts by focusing on chemical and physical modification of the treated media, such as evaporation, temperature, acidification, increase of osmolality, dissolved oxygen and accumulation of  $H_2O_2$  and NO-related compounds. Second aim was to evaluate the viability and proliferation rate of human dermal fibroblasts (HDFs) after treatment with the  $\mu$ APPJ to conclude to possible wound healing effects.

## 2. Materials and methods

### 2.1 Materials

#### 2.1.1 Cells

##### Human Fibroblasts

established from skin tissue of 8 patients  
undergoing abdominoplasty

*7 female and 1 male patients*

*39-75 years old, mean 52.4±15.3 years*

*Used with donor consent and approval  
of the Ethics Commission of Düsseldorf  
University (Study No. 3634)*

#### 2.1.2 Common materials

0.5 ml Tube *Safe-Lock Tubes™*

Eppendorf AG (Hamburg, Germany)

1.5 ml Tube *Safe-Lock Tubes™*

Eppendorf AG (Hamburg, Germany)

2 ml Tube *Safe-Lock Tubes™*

Eppendorf AG (Hamburg, Germany)

15 ml Conical Tube *No. 188171*

GREINER bio-one (Solingen, Germany)

24-Well Plates *Cellstar® Tissue*

*Culture Plates*

GREINER bio-one (Solingen, Germany)

50 ml Conical Tube *No. 227261*

GREINER bio-one (Solingen, Germany)

Counting Chamber *Neubauer*

BRAND GmbH + CO KG (Wertheim,  
Germany)

Cryo Tubes *Cryos™ 2 ml*

GREINER bio-one (Solingen, Germany)

## Materials and methods

Cell Culture Flask 75 cm <sup>2</sup> <i>Cellstar</i> ®	
<i>Cell Culture Flasks Red Filter Cap</i>	GREINER bio-one (Solingen, Germany)
Cell Culture Flask 175 cm <sup>2</sup> <i>Cellstar</i> ®	
<i>Cell Culture Flasks Red Filter Cap</i>	GREINER bio-one (Solingen, Germany)
Gastight Syringe Series 1700	Hamilton Bonaduz AG (Bonaduz, Switzerland)
Pasteur Pipettes ISO 7712	BRAND GmbH + CO KG (Wertheim, Germany)
Petri Dishes <i>Dish 100</i>	SARSTEDT TC (Nümbrecht, Germany)
Pipette Tips <i>TipOne</i> ®	Star lab group (Hamburg, Germany)
Pipette Tips Filtered 50 µl <i>TipOne</i> ®	Star lab group (Hamburg, Germany)
Pipette Tips Filtered 100 µl <i>TipOne</i> ®	Star lab group (Hamburg, Germany)
Pipette Tips Filtered 200 µl <i>TipOne</i> ®	Star lab group (Hamburg, Germany)
Microscope Slides No. 11101	Engelbrecht (Edermünde, Germany)
5 ml Stripette <i>Costar</i> ®	Sigma-Aldrich (Bensalem, PA, USA)
10 ml Stripette <i>Costar</i> ®	Sigma-Aldrich (Bensalem, PA, USA)
35 ml Stripette <i>Costar</i> ®	Sigma-Aldrich (Bensalem, PA, USA)

### 2.1.3 Cell culture

Bovine Serum Albumin Fraction	PAA (Paschin, Austria)
Calcium Chloride Dehydrate	Sigma-Aldrich (St. Louis, MI, USA)
CellTiter-Blue® Cell Viability Assay	Promega (Madison, WI, USA)
Collagenase Type CLS 255 U/mg	Biochrom (Berlin, Germany)
D-(+)-Glucose	Sigma-Aldrich (St. Louis, MI, USA)
DMEM 1g/L Glucose	PAN Biotech (Aidenbach, Germany)

## Materials and methods

Dispase II	Sigma-Aldrich (St. Louis, MI, USA)
HEPES	Sigma-Aldrich (St. Louis, MI, USA)
Sodium Chloride (0,9 %)	Braun (Melsungen, Germany)
Penicillin (100x)	PAA (Paschin, Austria)
Phosphate Buffered Saline	Invitrogen (Carlsbad, MA, USA)
Potassium Chloride	Roth (Karlsruhe, Germany)
L-Glutamine 200 mM (100x)	Gibco (Karlsruhe, Germany)
Streptomycin (100x)	PAA (Paschin, Austria)
SeraPlus Special Processed FBS	PAA (Paschin, Austria)
Sodium Chloride	VWR (Radnor, PA, USA)
Trypsin/EDTA Solution (10x)	Biochrom (Berlin, Germany)

### 2.1.4 Chemiluminescence detection (Nitrate, Nitrite)

Hydrochloric Acid (1.0N)	Carl Roth GmbH + Co. KG (Karlsruhe, Germany)
Sulphuric Acid (1.0N)	Carl Roth GmbH + Co. KG (Karlsruhe, Germany)
Sodium Nitrite	VWR (Radnor, PA, USA)
Sodium Nitrate	VWR (Radnor, PA, USA)
Vanadium(III) chloride	Sigma-Aldrich (St. Louis, MI, USA)

### 2.1.5 Hydrogen peroxide and catalases control

Catalase	Carl Roth GmbH + Co. KG (Karlsruhe, Germany)
----------	--

## Materials and methods

Hydrogen Peroxide Carl Roth GmbH + Co. KG (Karlsruhe, Germany)

### 2.1.6 Hydrogen peroxide photometry

Titanium Oxalate Sigma-Aldrich (St. Louis, MI, USA)

### 2.1.7 Fluorescence photography

Fluorescein Diacetate Thermo Fisher Scientific (Waltham, MA, USA)

Hoechst 33342 Solution Thermo Fisher Scientific (Waltham, MA, USA)

Propidium Iodide Thermo Fisher Scientific (Waltham, MA, USA)

### 2.1.8 Operative equipment

Scalpel Medico Care B.V. (Numansdorp, Netherlands)

Surgical Pincer Medico Care B.V. (Numansdorp, Netherlands)

Surgical Scissor Medico Care B.V. (Numansdorp, Netherlands)

## Materials and methods

### 2.1.9 Devices and equipment

Bench <i>HERAsafe</i> ®	Thermo Fisher Scientific (Waltham, MA, USA)
Centrifuge <i>Heraeus Megafuge 16 R</i>	Thermo Fisher Scientific (Waltham, MA, USA)
Cryo Rate Freezer <i>Cryo-Froster Mr. Frosty</i>	Schmidt Laborgeräte und Umweltsimulationen (Pressbaum, Austria)
COST Reference Microplasma Jet <i>Mirco-Scaled Atmospheric Pressure Plasma Jet</i>	Ruhr-Universität Bochum (Bochum, Germany)
Digital Thermometer <i>GMH3239</i>	Greisinger Electronic (Regenstauf, Germany)
Digital Dissolved Oxygen/Temperature Electrode <i>HI764080</i>	Hanna Instruments (Carrollton, TA, USA)
Helium Gas <i>99.99 % Purity</i>	Linde (Munich, Germany)
Heating Bath <i>Drybath</i>	Thermo Fisher Scientific, (Waltham, MA, USA)
Fluorescence Microscope <i>Axioplan Epi-Fluoreszenz</i>	Carl Zeiss AG (Oberkochen, Germany)
Incubator <i>NuAire DH Autoflow CO<sub>2</sub> Water-Jacketed Incubator</i>	Nuair Autoflow (Plymouth, MA, USA)
Light Microscope <i>Axiovert 40</i>	Carl Zeiss AG (Oberkochen, Germany)
NO/NO <sub>x</sub> -Analyzer <i>CLD 88</i>	Ecophysics (Munich, Germany)

## Materials and methods

NO/NO <sub>x</sub> -Analyzer <i>CLD 88 e</i>	Ecophysics (Munich, Germany)
NO/NO <sub>x</sub> -Analyzer <i>CLD 822r</i>	Ecophysics (Munich, Germany)
Optical Emission Spectroscope <i>HR 4000</i>	Ocean Optics (Duvien, Netherlands)
pH-Meter <i>Calimatic 766</i>	Knick (Berlin, Germany)
Multiparameter pH-Meter <i>HI2020-Edge</i>	Hannah Instruments (Carrolton, TA, USA)
pH-Electrode <i>InLab-Micro</i>	Mettler-Toledo (Giessen, Germany)
Photometer <i>Specord 205</i>	Analytik Jena AG (Jena, Germany)
Pipettboy <i>Accu-Jet® Pro</i>	Brand (Wertheim, Germany)
Pipettes <i>Research® Fix</i>	Eppendorf AG (Hamburg, Germany)
Power Supplier <i>Power Source</i>	VWR (Radnor, PA, USA)
Mass Flow Controller <i>FC280S</i>	Millipore-Tylan (Bedorf, MA, USA)
Multilabel Plate Reader <i>VICTOR3™</i>	
<i>V Multilabel Counter Model 1420</i>	PerkinElmer (Waltham, MA, USA)
Scale <i>KenABJ Log NoA01 Electronic</i>	
Balance Typ <i>ABJ 2204</i>	Kern und Sohn GmbH (Balingen, Germany)
Vortex Mixer <i>IKA® RET</i>	Heidolph (Schwabach, Germany)
Wobble Roller Mixer <i>RM5-V 1750</i>	Ingenieurbüro CAT M. Zipperer GmbH (Ballrechten-Dottingen, Germany)
<b>2.1.10 Software</b>	
Microsoft Excel	Microsoft Corporation (Redmond, WA, USA)

## Materials and methods

Microsoft PowerPoint	Microsoft Corporation (Redmond, WA, USA)
Microsoft Word	Microsoft Corporation (Redmond, WA, USA)
Origin 8	OriginLab Corporation (Northampton, MA, USA)
PowerChrom™	eDAQ (Deinstone East, Australia)
PRISM 8	Graphpad Software, Inc.(San Diego, CA, USA)
ZeissAxioVision	Carl Zeiss AG (Oberkochen, Germany)

### 2.2 Methods

#### 2.2.1 Cell culture

The human fibroblasts were cultivated in a CO<sup>2</sup>-Incubator under standard conditions (37 °C, 5 % CO<sub>2</sub>, 90 % humidity). The cells were accomplished either in 75 cm<sup>2</sup> or in 175 cm<sup>2</sup> Cell Culture Flasks. Every single step of treatment has been processed at a laminar flow cabinet under sterile requirements. The adherent growing fibroblasts sustained with Dulbecco's modified Eagles's Medium (DMED), enriched with 100 U/ml penicillin (Pen), 100 µg/ml streptomycin (Strep) and 10 % (v/v) fetal calf serum (FCS). The plastic-adherent cells were undergoing media changes every three days.

#### 2.2.2 Cell subculturing

To enable the confluent cells to grow further in other cell culture flasks or 24-Well plates they were undergoing a passaging process. To remove the adherent fibroblasts from the flasks fresh augmented medium and trypsin were placed in a 37 °C water bath to warm up. The consumed medium had to be siphoned by an aspirator. The blank cells were washed two times with calcium and magnesium free phosphate buffered saline (PBS). After aspirating the PBS 5-10 ml warm trypsin/EDTA were given to the still adherent fibroblasts in the cell culture flasks to detach them. The flasks were put into the incubator under standard cultivation conditions for 5-7 min until most of the cells are released from the surface. A longer incubation time must be avoided to forestall cell death. To neutralize the trypsin/EDTA the same amount of modified medium was added to the cell suspension. Following the fluid was transferred to a 50 ml Falcon. After centrifugation for 5 min under 300x g the supernatant above the pellet was syphoned and 10 ml new medium was given to the cells. Hence the human fibroblasts were resuspended with a 1000 µl pipette until an approximately clear fluid was given. Hereafter one could enumerate the cells and/or to passage them into new cell culture flasks to facilitate more process of growth.

## Materials and methods

To enable the enumeration of fibroblasts 10 µl of the cell suspension was given onto a Neubauer counting chamber. Once the coverslip plate was vacuumed to the Neubauer counting chamber one could count the number of cells on four quarters by microscoping. To determine the number of fibroblasts in 10 µl cell suspension one could calculate the arithmetic average of all four quarters. Most recently the nearly exact number of cells was calculated by this formula:

$$\text{Cell density} = \text{dilution number} * \frac{\text{counted cell number}}{4} * 10^4 * \text{ml}^{-1}$$

After the enumeration, the accurate number of cells in each amount of suspension could be stated. Hence it was possible to put the exactly fitting and required number of cells into 24-Well plates – or otherwise if the demanded amount of fibroblast was not given the suspension could be transferred back to cell culture flasks.

### 2.2.3 Cryopreservation

To preserve fibroblasts from a current cell lines to harness them in future experiments they have been cryopreserved in 2 ml Cryo Greiner tubes with 10 % DMSO and 90 % FCS. Immediately after passaging 500,000 – 1,000,000 cells were inoculated to the suspension and the tubes have been placed in cry freezing buckets filled with isopropanol to ensure a cautious freezing. After freezing for 4 h down to -80 °C they were sided in an ordinary box to store for an extended period of time.

To defrost cells from former fibroblast cultures they were thawed in a 37 °C water bath until the suspension was partially liquid. Following the tubes were removed from the water bath and the fluid was gently resuspended as far as the entirety solution was molten. Modified medium was added, and the tubes were centrifuged (300x g for 5 min). The supernatant was aspirated and replaced by fresh medium and the cell pellet was resuspended. Finally, the medium with defrosted cells were placed in 75 cm<sup>2</sup> cell culture flasks with 30 ml DMED and the thawing was accomplished. The cell culture flasks were stored in an incubator by named standard conditions.

### 2.2.4 Cell isolation

Removed skin samples were set in medium straight after surgery and carried in cooled and sterile boxes to the laboratory. After removing the medium the skin was put in a petri dish to be cut in small pieces with a scalpel and pincers. These pieces were placed in a 50 ml tube with 5 - 10 ml Dispase II solution and incubated overnight at 4 °C. The next day epidermis und dermis were separated.

Exclusively the dermis containing the fibroblasts was put in another 50 ml tube with collagenase buffer for 45-60 min at 37 °C in a tempered shaker. The epidermis could be used to isolate keratinocytes for other assays and was given away. The solution together with the dermis samples were put in a vortex machine thus the cells in the liquid were blended. After that, the solution was given into a sieve (50-100 µM) to drain the fibroblasts from the samples. Carefully the skin samples were pressed in the filter and washed with PBS to achieve the best possible result and gain the most fibroblasts. The acquired solution was put in a new 50 ml tube and centrifuged with 300x g for 10 min. The supernatant was removed, and the cell pellet resuspended with 10 ml new DMEM. Finally, the isolated fibroblasts were given into cell culture flasks and put into the incubator (37 °C, 5 % CO<sub>2</sub>) to grow.

<b>Solution</b>	<b>Ingredients</b>
Dispase II Solution	0.1 % Dispase II 5 % 1M Hepes buffer solution <i>ad.</i> PBS
Collagenase buffer	100 mM Hepes 120 mM NaCl 50 mM KCl 1 mM CaCl <sub>2</sub> 5 mM Glucose

**Table VII Composition of used solutions.** Described are the different agents and their amounts of the Dispase II solution and the Collagenase buffer.

### 2.2.5 Plasma/CAP source and its characterization

The capacitively coupled microplasma jet ( $\mu$ APPJ) contained two stainless steel electrodes with a length of 30 mm and a width of 1 mm. The plasma was emplaced in a gap of 1 mm between the electrodes with a volume of  $1 \times 1 \times 30 \text{ mm}^3$ . The jet holder consisted the electric connection, the gas connector and the gas feed tubing. However, the whole device embodied an electrode stack with 1.5 mm thick quartz panes that enclosed the plasma volume (identical to the COST reference electrode head [194]). One electrode was provided by a power supply (13.56 MHz,  $1 < W$ ), whereas the other electrode was grounded. The operating range of the  $\mu$ APPJ reached from 0.25 slm up to 1.4 slm and was generated by a helium gas flow, but small admixtures of molecular oxygen ( $>0.6 \%$ ) were possible [90]. A mass flow controller monitored the helium gas flow. Furthermore, an optical emission spectroscopy with an optical fiber was applied to determine the plasma under experimental conditions.

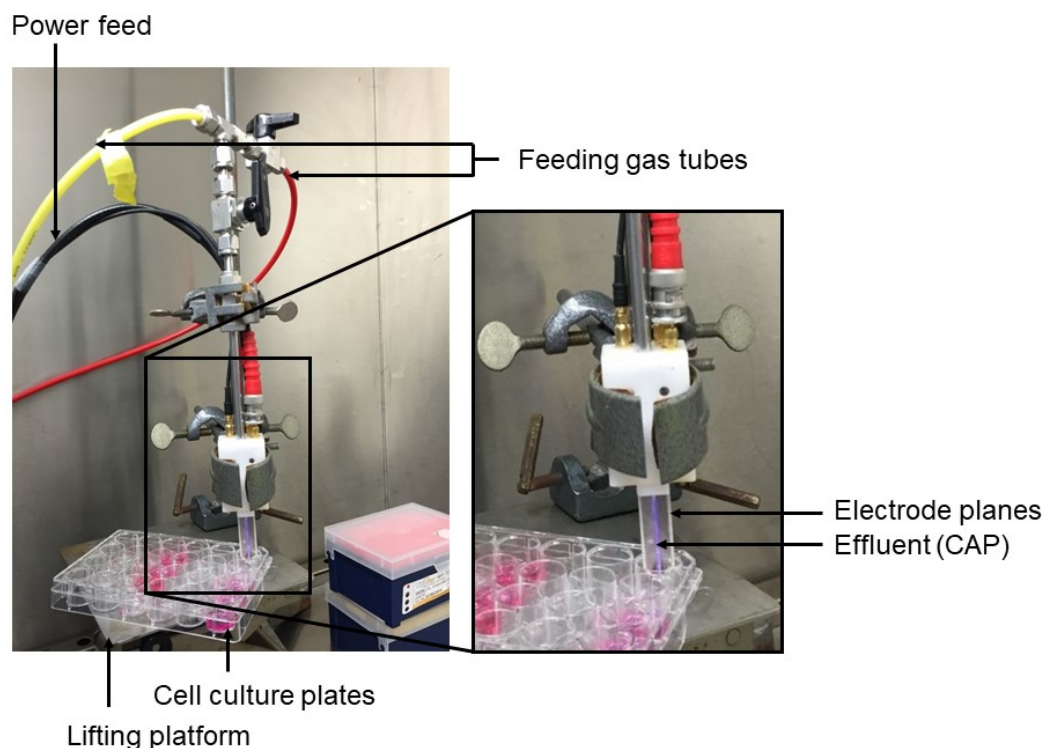


**Fig. V Experimental build up of the jet holder.** Through the feeding tubes helium gas is delivered between the electrode planes and here conducted to the plasma phase. The device is powered through the power feed. The samples to treat were presented on a lifting platform right to the effluent tip of the  $\mu$ APPJ.

### 2.2.6 Treatment methods

For exposure assays the HDF were placed at a cell density of  $2.5 \times 10^4$  in 24-well plates two days before experiments to attach with needed DMEM. The HDF were carefully washed with 500  $\mu\text{l}$  PBS prior treatment by the  $\mu\text{APPJ}$  to facilitate a pure and uniformly exposure. Subsequent 500  $\mu\text{l}$  PBS was given to the HDFs to avoid evaporation due to direct contact to ambient air. The gap between electrode end and the fibroblasts at the bottom of the 24-well plate was kept as 7mm. Hence the distance between the surface of the PBS and the nozzle of the jet was 5 mm (see figure VI).

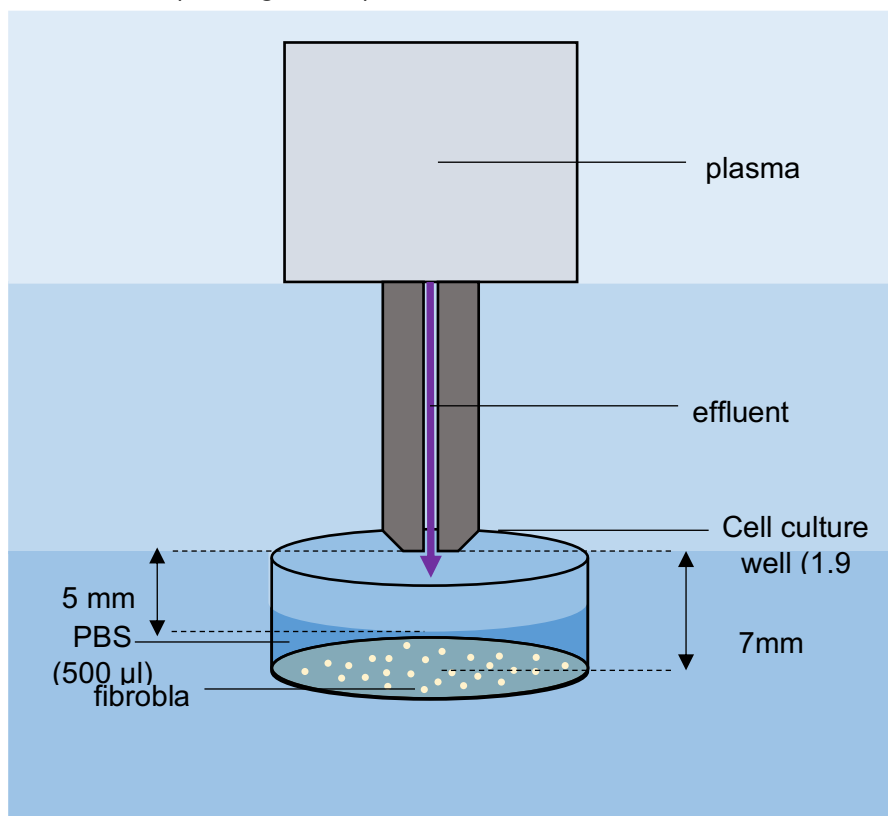


**Fig. VI Schematic build up of direct treatment.** Distance between nozzle and bottom of the well-plate is kept as 7 mm, the distance between PBS surface and nozzle as 5 mm. This overview can be transferred to other treatment assays excluding the indirect fibroblasts - or the  $\text{H}_2\text{O}_2$ -Control-Assay (own illustration).

For direct treatment, the cells were treated directly with a helium plasma flow of 0.25 slm for different lengths of time (1, 2.5, 5 and 10 min). Additionally, a control sample was untreated, and another sample was treated for 10 min with helium gas (0.25 slm). Besides, as a control to determine the effect of  $\text{H}_2\text{O}_2$ ,  $\text{H}_2\text{O}_2$  catalase (1000 U/ml) was added to the buffer prior the 10 min helium plasma exposure. After each exposure, PBS was substituted with fresh medium and the cells were incubated under standardized conditions.

## Materials and methods

For indirect treatment, the 500  $\mu$ l of PBS was separately treated from the cells with two helium plasma flows (0.25 and 1.4 slm) for various times (1, 2.5, 5 and 10 min). The assay was divided into three exposure lines. In the first treatment row buffer was treated with helium plasma (1.4 slm) and was given undiluted to the cells for indicated times. In the second row the plasma treated (1.4 slm) PBS was replenished up to 500  $\mu$ l to restore the loss of liquid due to evaporation. In the third assay row the buffer treated by 0.25 slm with helium plasma was also refilled with untreated PBS up to 500  $\mu$ l. Immediately after exposure and contingent replenishment each treated buffer was transferred to the HDFs on the 24-well plate to incubate them for 1, 3, or 5 min. For each highest incubation time (5 min) one cell sample remained completely untreated and to another sample catalases (1000 U/ml) was added before transferring the buffer to the HDFs. Subsequently after incubation the PBS of each sample was substituted with fresh MDEM.

To measure the effect of  $H_2O_2$  on cells, that is also feasibly produced while plasma treatment, and the protective characteristics of catalases, an assay named “ $H_2O_2$  control” was conducted. In this assay row hydrogen peroxide was diluted from 100 mM to 1  $\mu$ M in steps by the factor of 10 with PBS, hence 500  $\mu$ l of buffer solutions resulted. Solutions of 1  $\mu$ M, 10  $\mu$ M, 100  $\mu$ M, 1mM and 10 mM were given for 5 min to prepared HDFs, following they were incubated under standardized conditions with fresh medium. Moreover, 1000 U/ml catalases were inoculated to 10  $\mu$ M, 100  $\mu$ M and 1mM  $H_2O_2$  solutions and given to the HDFs for 5 min. Subsequently, the PBS was substituted with fresh medium and put into the incubator.

After each assay the cell viability were determined using the CellTiter-Blue® Cell Viability Assay as described below. The measurements were conducted on the first, the fourth and the eighth day after treatment by the  $\mu$ APPJ.

### 2.2.7 CellTiter- Blue® cell viability assay

The CellTiter-Blue® Assay was used to establish the cell viability of cells. The CellTiter-Blue® solution contained the indicator dye resazurin. Living cells

## Materials and methods

can metabolize resazurin to resofurin. Both dyes have diverse absorbance maxima. Hence a spectrofluorometer could distinguish living and dead cells by detecting the different dyes. The utilized spectrofluorometer was the VICTOR X Multilabel Plate Reader of the company PerkinElmer containing a wavelength measurement of 590 nm.

CellTiter- Blue® Cell Viability Assay was used in my thesis to determine the direct toxicity after cold atmospheric plasma treatment and potential proliferation variances. The dye was mixed 1:20 with DMED and 350 µl were given to the treated cells. These were placed for one hour in the CO<sub>2</sub> incubator (37 °C, 5 % CO<sub>2</sub>) to incubate. To ensure the results 100 µl of every dilution were placed on 96-well plates twice and put in the spectrofluorometer. Moreover, the used cell cultures were washed with PBS und supplied with fresh medium after measurement to use them in further assays.

### 2.2.8 Fluorescence microscopy

HDFs were seeded at a cell density of  $2.5 \times 10^4$  in 24-well plates two days before experiments to attach. These samples were exposed to helium gas flows of 0.25 and 1.4 slm for 0, 1 and 10 min. Prior and after treatment the cells were observed by a Zeiss light microscope to observe possible detachment or cell deformation. Directly after the fluorescence dyes (Hoechst 33342, fluorescein diacetate and propidium iodide, each dye 0.5 µg/ml) were inoculated and the HDF were incubated for 3-5 min by standard conditions (37 °C, 5 % CO<sub>2</sub>). Subsequently the dyes were replaced with 500 µl PBS and the cells were analyzed using a fluorescence microscope. Feasible results were documented by using ZeissAxioVision.

### 2.2.9 Measurement of hydrogen peroxide

To determine a specific amount of hydrogen peroxide in a solution a photometer with a wavelength of 400 nm was used. First a stock solution of potassium titanium oxide oxalate dehydrate (35.4 mg/ml) with 2 M sulphuric acid

## Materials and methods

was prepared. Specific amounts of hydrogen peroxide were added to 200  $\mu\text{l}$  untreated PBS with 200  $\mu\text{l}$  stock solution. Following the solution was measured with the photometer to gain a specific calibration curve for further measurements [195].

500  $\mu\text{l}$  PBS was treated with non-thermal plasma. 150  $\mu\text{l}$  of this solution was given to 50  $\mu\text{l}$  untouched PBS and 200  $\mu\text{l}$  stock solution. The dilution of 1:4 was necessary because otherwise the determined amount of hydrogen peroxide could be too high to measure. If hydrogen peroxide emerged it induced a reaction with the potassium titanium oxide. An evidence of an occurred reaction was a yellowish color that could be detected by the mentioned photometer. The increasing hydrogen peroxide concentration was congruent with the absorption of light. Hence, with the aid of the determined calibration curve the particular amounts of hydrogen peroxide in treated samples could be defined. However, to measure possible hydrogen peroxide accumulation prior and after helium gas or plasma treatment 500  $\mu\text{l}$  of PBS were treated with 0.25 and 1.4 slm of helium gas/CAP for different times (0-10 min).

### 2.2.10 Reductive gas-phase chemiluminescence

To quantify the NO-content of treated samples an iodine/iodide-based assay was deployed by using two NO-analyzer (CLD 88/88e). Each analyzer consisted a reflux condenser to release the gaseous molecules of NO to drive them into the NO-analyzer.

The first condenser was charged with a 35 ml solution of potassium iodide, iodine and a 96 % ethanoic acid, the second with a 35 ml mixture of vanadium chloride solved in 1 M HCl (1 % VaCl). The iodine solution was heated up to 65 °C and the VaCl solution to 94.7 °C by warm water baths. Subsequently CO<sub>2</sub> passed through the reflux condensers to transport gaseous NO to a cooling trap filled with 1 M NaOH and to run further to the reaction chambers of both NO-analyzers. There NO reacted with ozone to nitrogen dioxide (NO<sub>2</sub>). During this reaction energy in form of light was emitted that could be determined by the NO-analyzers. An exact amount of nitrate and nitrite (100  $\mu\text{M}$ ) was quantified with

## Materials and methods

gas-phase chemiluminescence to facilitate accurate measurements (see figure VII).

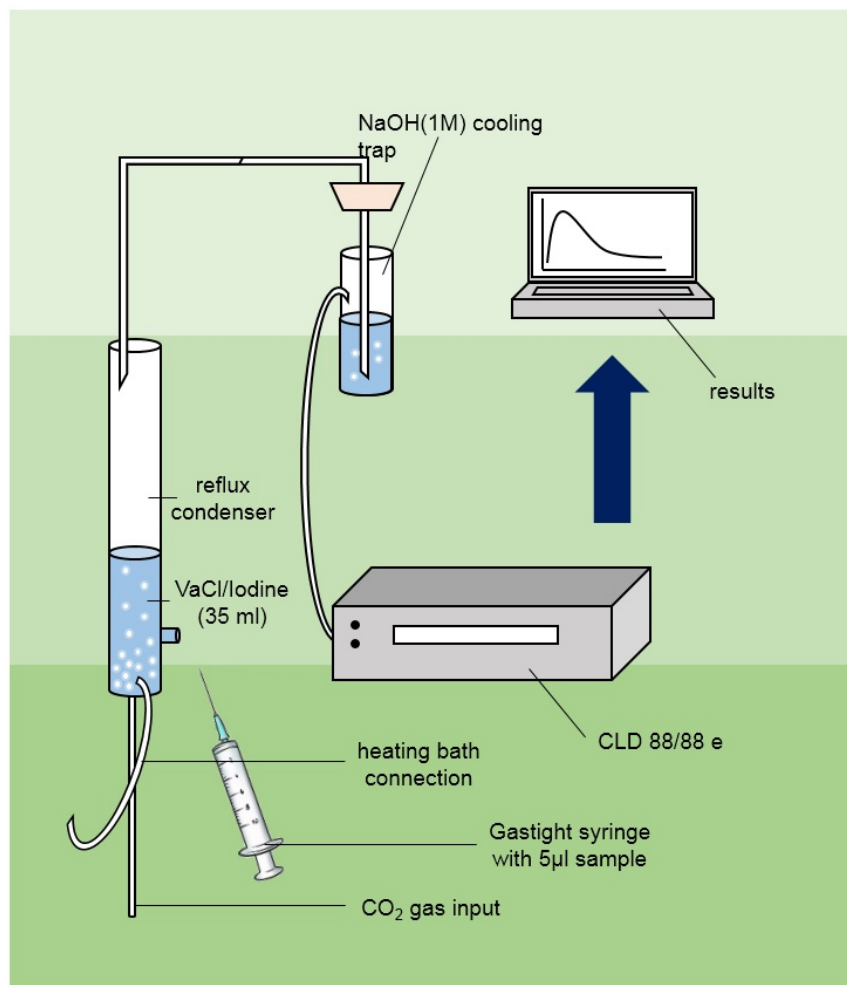


**Fig. VII Schematic buildup of reductive gas-phase chemiluminescence.** After inoculating the sample, the reactant flows through the reflux condenser to the cooling trap and further to the analyzer, in which it reacts with ozone to NO. This is detected and gets recorded by Origin 8 (own illustration).

5 µl of the exposed samples were inoculated with a 10 µl gastight syringe through a gastight membrane into the reaction solution. Recording and analysis were conducted by using Origin 8.

### 2.2.11 Nitric oxide and nitric dioxide Assay

The concentrations of nitrogen oxides (NO<sub>2</sub>) and nitric oxide (NO) were determined in the gas phase at the outlet of the µAPPJ by the NO/NO<sub>x</sub>-analyzer CLD 822r operated with an inflow of 0.025 slm. The optical emission was

## Materials and methods

measured about 1 mm from the electrode end of the jet that was operated with helium gas flow of 0.25 slm and 1.4 slm.

### 2.2.12 pH-Value assay

To detect possible pH-value varieties prior and after plasma treatment 500  $\mu$ l phosphate buffered saline (PBS) was given multiple times onto a 24-well plate and were treated with different gas and helium plasma flows (0.25 and 1.4 slm) for various durations (0-10 min). To determine a calibrated pH meter and a pH electrode) were used.

### 2.2.13 Evaporation assay

The evaporation rate was measured by determining the different liquid volumes prior and after gas treatment. Therefore, various amounts of PBS (250, 500, 750, 1000  $\mu$ l) were given onto a 24-well plate and every sample was treated by the  $\mu$ -APPJ with 0.25 and 1.4 slm helium gas for 0, 1, 2.5, 5 and 10 min. To detect variances a micro scale and a pipette were used.

### 2.2.14 Temperature assay

In the preliminary experiments, the temperature of treated buffer in various amounts (250, 500, 750, 1000  $\mu$ l) in cell culture plates (24-well) before and after  $\mu$ APPJ treatments or gas control (flow rates 0.25 slm, 1.4 slm) was measured by using a digital thermometer after different treatment intervals (0 min, 5 min, 10 min).

### 2.2.15 Dissolved oxygen assay

A multiparameter pH-Meter and a digital dissolved oxygen/temperature electrode were used to measure the oxygen saturation of treated and untreated

## Materials and methods

PBS buffer. 500  $\mu$ l of PBS were put on a 24-well plate and treated concisely with two different gas flows (0.25 and 1.4 slm) for 0-10 min.

### 2.2.16 Statistical analysis

Significant differences were evaluated using either paired two-tailed Student's t-test or ANOVA followed by an appropriate post-hoc multiple comparison test (Tukey method). A  $p < 0.05$  was considered as significant.

## 3. Results

### 3.1 Plasma characterization

The comparison of spectra taken with low (0.25 slm) and high (1.4 slm) flows (see figures VIII, IX) was accomplished in collaboration with Schulz von der Gathen and co-workers. The displayed results are published here with his official permission. These results showed, apart from the lines expected by the operating gases (helium and oxygen), other lines that could be identified. In particular, atomic hydrogen (H-alpha) and neutral and ionic molecular nitrogen as well as NO and hydroxyl (OH) could be detected. For the higher flows, the NO as well as the neutral nitrogen molecules were severely reduced.

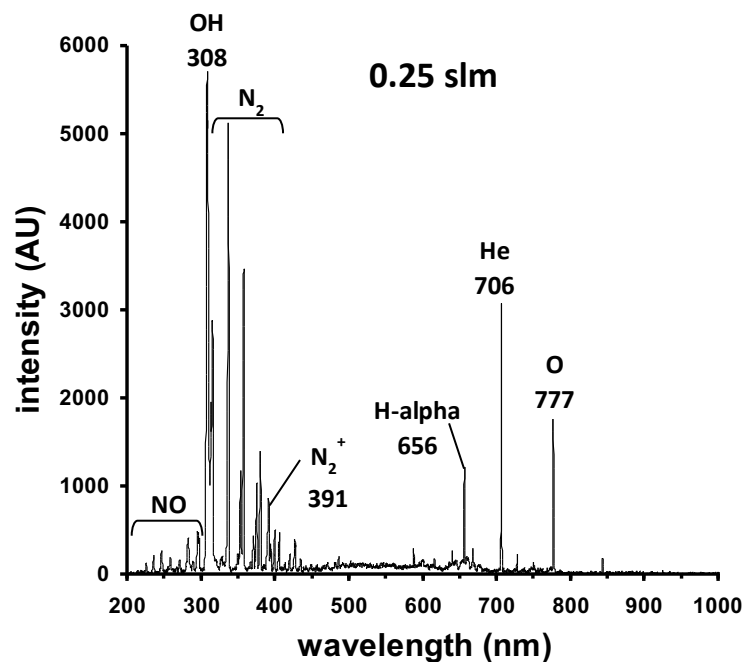


*Fig. VIII Characterization of CAP at 0.25 slm flow. The OES spectra of plasma generated by  $\mu$ APP jet operated with helium gas flows of 0.25 slm showed other lines than the operated gases could be detected (H-alpha, NO, neutral and atomic nitrogen, hydroxyl).*

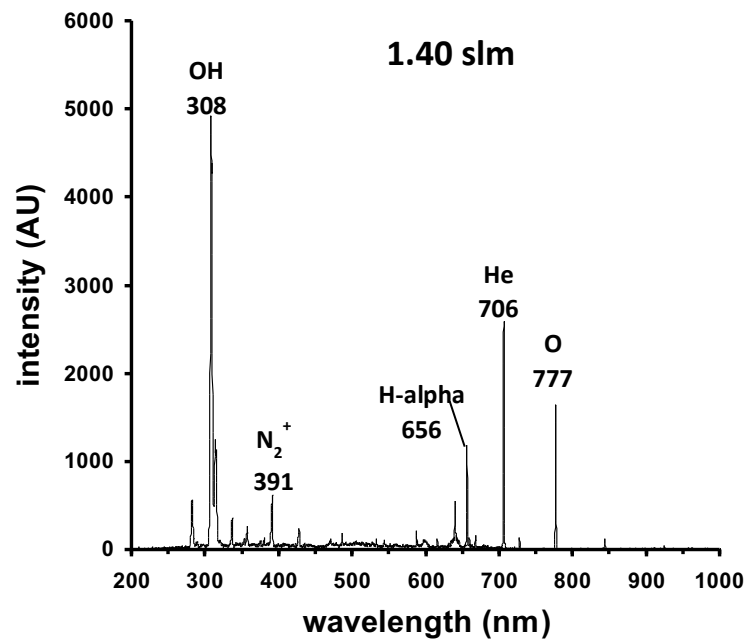


*Fig. IX Characterization of CAP at 1.40 slm flow. The OES spectra of plasma generated by  $\mu$ APP jet operated with helium gas flows of 1.40 slm showed other lines than the operated gases can be detected (H-alpha, NO, neutral and atomic nitrogen, hydroxyl). NO and neutral nitrogen were remarkable reduced at higher flow in comparison to CAP at 0.25 slm.*

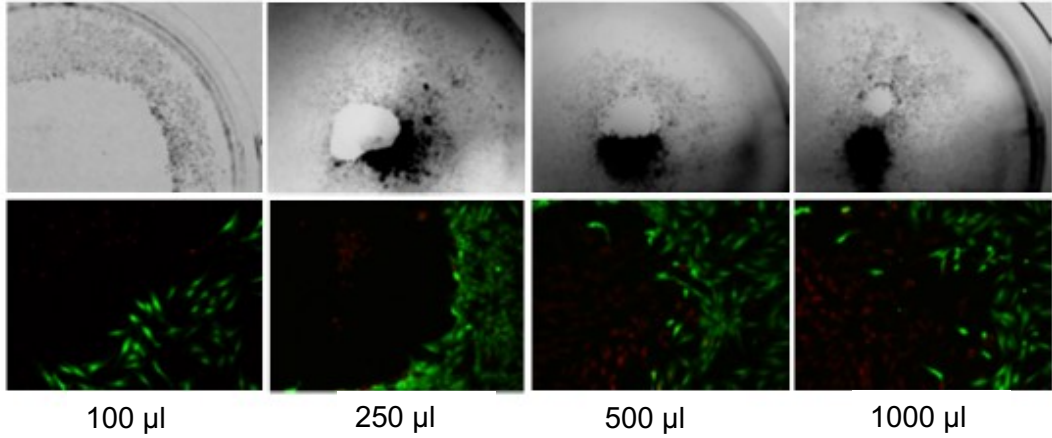
Measurements taken at the outlet of  $\mu$ APPJ directly by a NO/NO<sub>x</sub>-analyzer showed that there were substantial concentrations of nitric oxide and nitrogen dioxide in the effluent. The obtained concentration of nitric oxide was  $2.3 \pm 0.4$  ppm and nitrogen dioxide was  $1.7 \pm 0.2$  ppm, when using a gas flow of 0.25 slm. At a higher gas flow of 1.40 slm, the measured concentrations were  $0.8 \pm 0.2$  ppm and  $0.4 \pm 0.1$  ppm for NO or NO<sub>2</sub>, respectively.

### 3.2 Fluorescence microscopy of human dermal fibroblasts after helium gas treatment with the $\mu$ APPJ

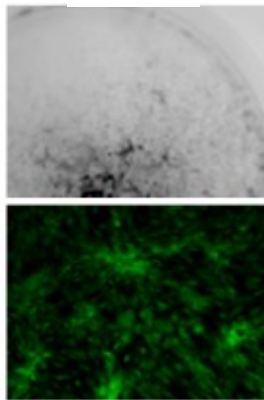
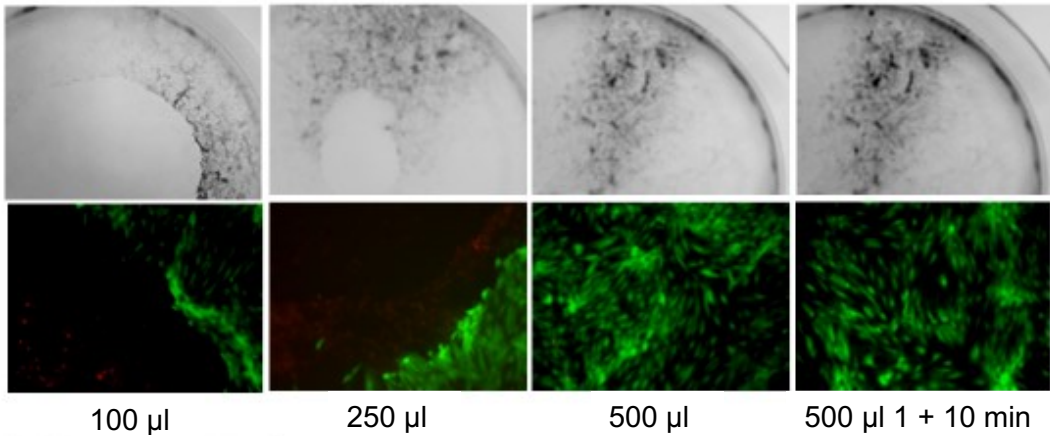
In Figure X are shown representative overviews of cell culture plates containing human dermal fibroblasts and their respective live staining images (fluorescein diacetate, propidium iodide) after treatment with helium applied by the  $\mu$ APPJ at a gas flow of 1.40 slm and 0.25 slm for one minute. At a gas flow of 0.25 slm and an amount of 500  $\mu$ l PBS no drying out effects could be displayed, whereas gas flow of 1.40 slm even with 1000  $\mu$ l PBS led to areas of reduced

viability of HDFs. We ensured the effect of no drying out at 0.25 slm gas flow and 500 ml PBS with a 10 min control.

**gas flow 1.4 slm**



**gas flow 0.25 slm**



**untreated control**

**Fig. X** *Overviews of cell culture plates of HDFs after gas flow treatment. Representative overviews of cell culture plates containing human dermal fibroblasts and their respective live staining images (fluorescin diacetate, propidium iodide) after treatment with helium for 1 min with a gas flow of 1.40 slm (images above) and 0.25 slm (images in the middle) as well as an untreated control (images below) are shown.*

### 3.3 Treatment of buffer with the $\mu$ APPJ

A treatment of the buffer with  $\mu$ APPJ as described in Figure VI led to significant evaporation, particularly when a higher gas flow was chosen (see figure X). We observed that the loss of buffer after 10 min of plasma treatment was nearly 50 %, when using a gas flow of 1.4 slm, whereas at 0.25 slm, the loss amounted to approximately 17 % of the original value of 500  $\mu$ l. Without plasma, the loss by helium gas flow alone was  $\sim$ 29 % and  $\sim$ 12 % for 1.4 slm and 0.25 slm, respectively.

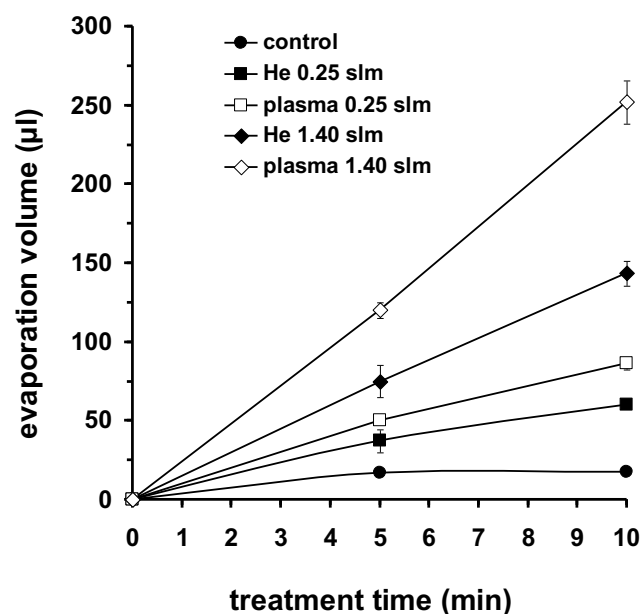


*Fig. XI Evaporation Assay. Evaporation due to direct treatment with the  $\mu$ APPJ regarding to a gas flow of 0.25 and 1.40 slm with and without plasma.*

We observed a strong decrease in buffer temperature during treatment. Under the chosen experimental conditions here with a starting temperature of 20  $^{\circ}$ C, the buffer temperature obtained was  $13.6 \pm 0.2$   $^{\circ}$ C colder after helium treatment with a gas flow of 1.40 slm after 10 min treatment. Applying CAP with 1.40 slm resulted in a temperature drop of  $7.9 \pm 0.3$   $^{\circ}$ C after 10 min treatment. The cooling effects by gas flow and evaporation were naturally lower when using a gas flow of 0.25 slm. The temperature of buffer obtained here after 10 min of treatment was  $6.0 \pm 0.4$   $^{\circ}$ C lower for the helium control and  $1.5 \pm 0.1$   $^{\circ}$ C lower for plasma.

## Results

The pH-changes of the treated buffer were shown in figure XII. Here, CAP treatments (10 min for 0.25 slm and 1.40 slm) of 500  $\mu$ l buffer induced a minor though a remarkable shift from pH 7.2 to pH  $\sim$ 7.0.

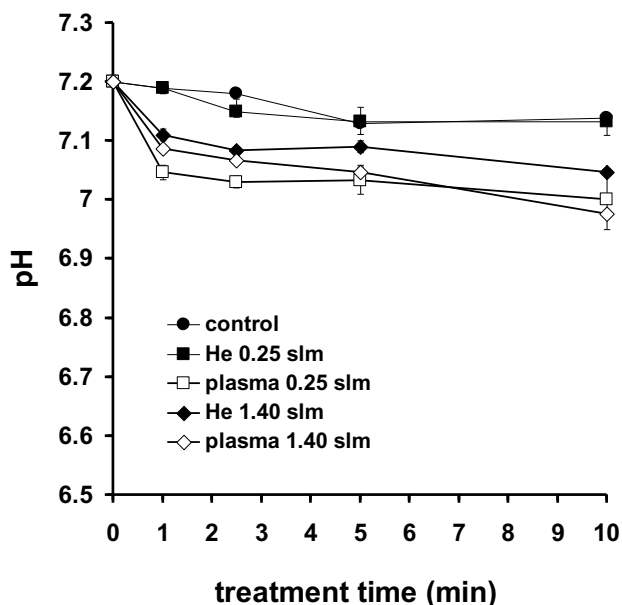


*Fig. XII pH-Value Assay. pH value change in buffer due to direct treatment with the  $\mu$ APPJ regarding to a gas flow of 0.25 and 1.40 slm with and without plasma.*

In addition,  $\mu$ APPJ treatment increased the amount of nitrite and nitrate in buffer (see figure XIII). Interestingly, the values obtained by using a gas flow of 0.25 slm were manifold higher than those by using 1.40 slm. For example, after 10 min of plasma treatment, comparative nitrite concentrations of  $161.4 \pm 27.7 \mu\text{M}$  (0.25

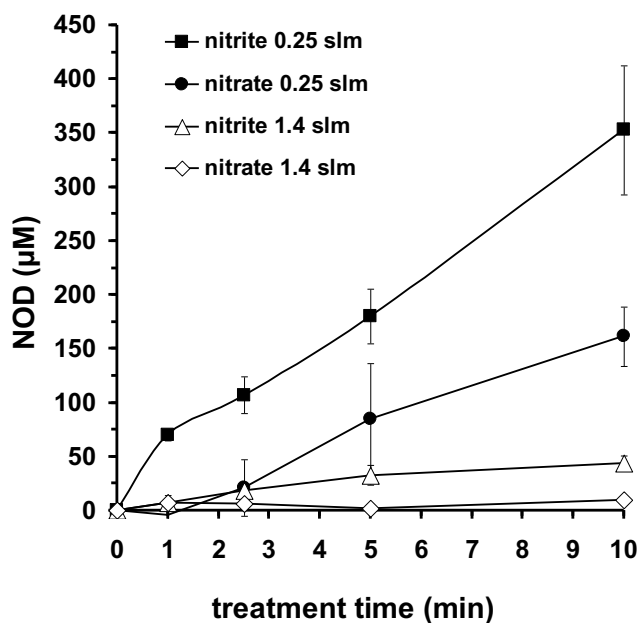


*Fig. XIII Reductive gas-phase chemiluminescence Assay. Concentrations of nitrite and nitrate in buffer after direct treatment with  $\mu$ APPJ regarding to a gas flow of 0.25 and 1.40 slm with plasma.*

## Results

slm) and  $9.7 \pm 2.4 \mu\text{M}$  (1.40 slm) and comparative nitrate concentrations of  $352.7 \pm 59.9 \mu\text{M}$  (0.25 slm) and  $44.1 \pm 6.6 \mu\text{M}$  (1.40 slm) were found.

However, as shown in figure XIV, gas treatment in our experimental setting led to a decrease in concentration of dissolved oxygen in the treated buffer. In particular, treatments using a gas flow of 1.40 slm showed losses of buffer volume up to 50 % and depleted oxygen completely after 10 min.

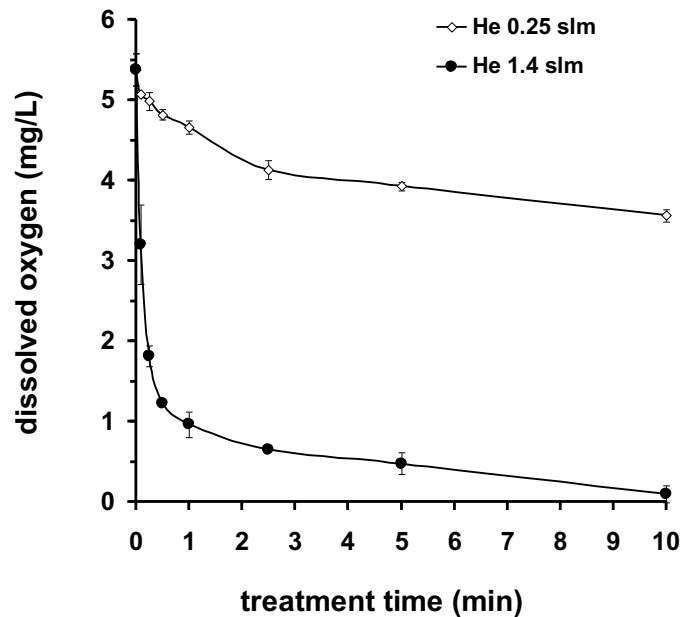


*Fig. XIV Dissolved oxygen Assay. Concentration of depleted oxygen in buffer after direct treatment with the  $\mu\text{APPJ}$  regarding to a gas flow of 0.25 and 140 slm without plasma.*

In addition, we investigated whether the  $\mu\text{APPJ}$  can produce relevant amounts of  $\text{H}_2\text{O}_2$  in the buffer. Here, we found a linear and treatment time-dependent increase of  $\text{H}_2\text{O}_2$  in the treated buffer. For example, a  $\text{H}_2\text{O}_2$  concentration of  $1265 \pm 148 \mu\text{M}$  was obtained after 10 min treatment using a gas flow of 1.4 slm whereas a 10-fold lower  $\text{H}_2\text{O}_2$  concentration ( $124 \pm 40 \mu\text{M}$ ) was found using 0.25 slm (see figure XV).

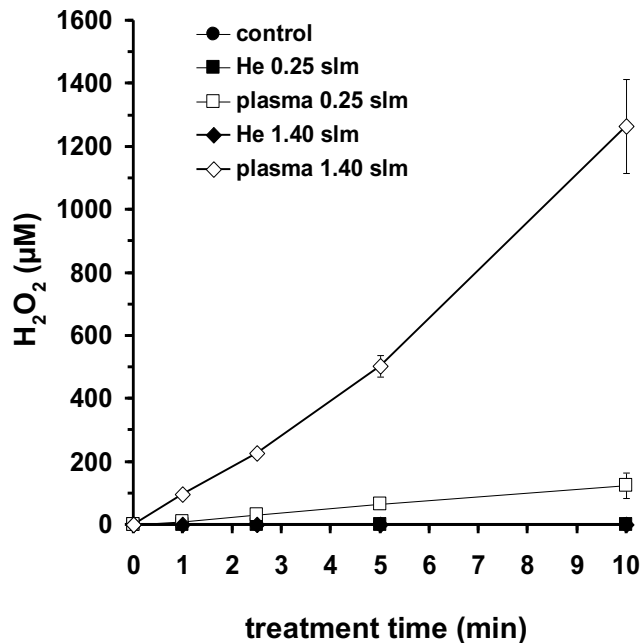


*Fig. XV Hydrogen peroxide Assay. Concentration of  $H_2O_2$  in buffer due to treatment with the  $\mu$ APPJ regarding to a gas flow of 0.25 and 1.40 slm with and without plasma.*

### 3.4 Treatment of human dermal fibroblasts in buffer with the $\mu$ APPJ

After evaluation of chemical/-physical modifications of plasma-treated buffer, the plasma-induced effect on human skin fibroblast (HDFs) were evaluated. Using a gas flow of 0.25 slm, we could not observe cell toxicity by drying off effects and the amount of evaporation was tolerable; thus, direct treatments of HDFs with  $\mu$ APPJ were performed with this gas flow. The direct plasma-treatment by using 0.25 slm reduced the cell viability (see figure XVI), which was significant only after a 10 min treatment ( $77 \pm 15 \%$ ). Regarding to the local drying out effects by applying helium gas flow of 1.4 slm (see Chapter 3.4), we performed only indirect plasma treatments on cells with this gas flow.

In indirect treatment a significant decrease in viability ( $49 \pm 29 \%$ ) were obtained only by using CAP-treated buffer (1.4 slm, 10 min) for a further 5 min period of incubation of the cells (Figure XVII). The toxic effect was weaker when the water-loss of the plasma-treated buffer was compensated by the addition of fresh buffer (Figure XVIII).

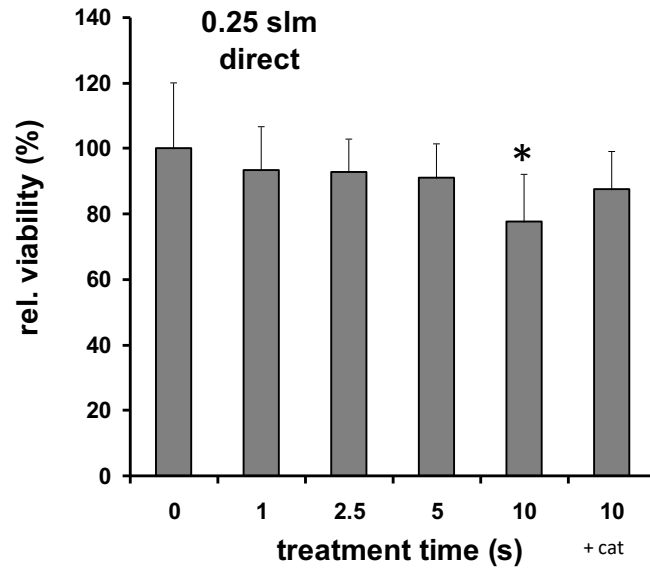


**Fig. XVI Direct treatment Assay.** Direct treatment of HDFs in 500 ml buffer with 0.25 slm plasma flow for 0, 1, 2.5, 5 and 10 min. In addition, a 10 min control with catalase was given.

It should be noted that the final H<sub>2</sub>O<sub>2</sub> concentration obtained was roughly reduced twofold by the dilution. By addition of catalase to scavenge H<sub>2</sub>O<sub>2</sub>, the observed reduction of viability could be brought down or totally diminished.

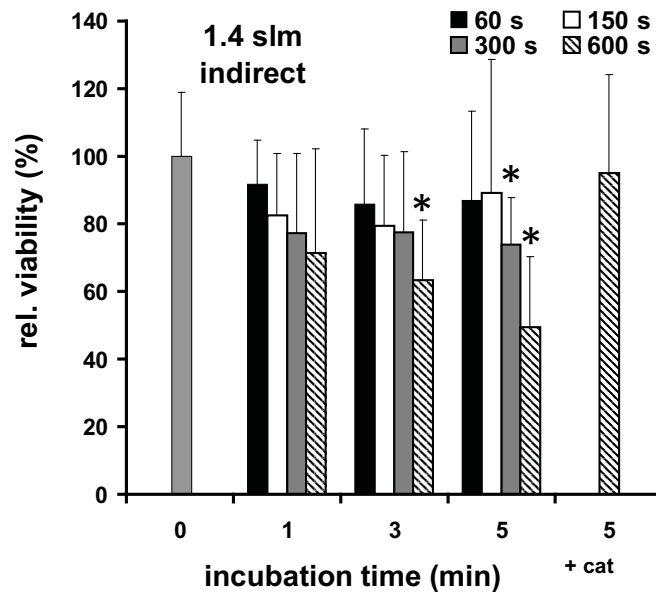


**Fig. XVII Indirect treatment with 1.40 slm without dilution Assay.** Indirect treatment of HDFs with 1.40 slm plasma with treat buffer for 1, 2.5, 5 and 10 min, following 0, 1, 3 and 5 min incubation time. In addition, a control with 10 min treated buffer and 5 min incubation time with catalase was given.

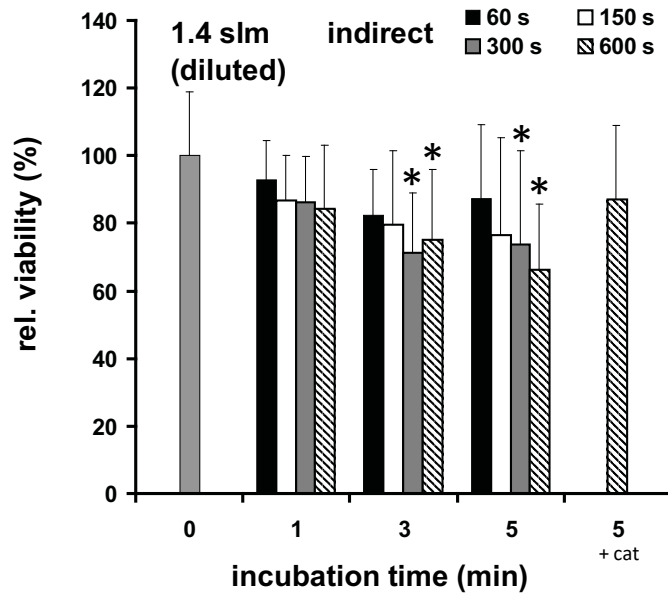


**Fig. XVIII Indirect treatment with 1.40 slm with dilution Assay.** Indirect treatment of HDFs with 1.40 slm plasma with tread buffer for 1,2.5, 5 and 10 min, following 0, 1, 3 and 5 min incubation time. The evaporation was compensated by addition of fresh buffer. In addition, a control with 10 min treated buffer and 5 min incubation time with catalase and compensation was given.

By using 0.25 slm, as shown in figure XIX, the indirect plasma-treatment showed a general but not significant decrease in cell viability ( $82 \pm 16$  %). Here, the addition of catalase could not reverse the decreasing effect of 0.25 slm plasma on cell viability ( $86 \pm 13$  %).

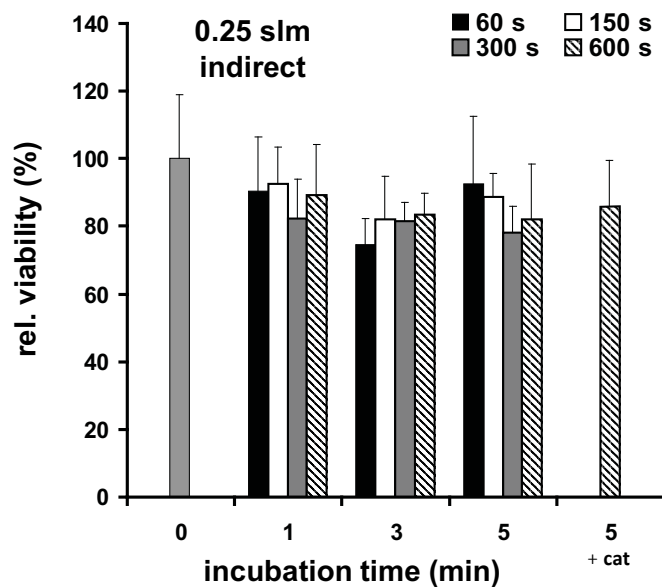


**Fig. XIX Indirect treatment with 0.25 slm Assay.** Indirect treatment of HDFs with 0.25 slm plasma with tread buffer for 1,2.5, 5 and 10 min, following 0, 1, 3 and 5 min incubation time. In addition, a control with 10 min treated buffer and 5 min incubation time with catalase and compensation was given.

## Results

As shown in Figures XX and XXI, the number of cells four days after indirect plasma treatment (1.4 slm, 5 min incubation) was significantly reduced in comparison to the controls. These effects could be diminished by the addition of catalase for scavenging H<sub>2</sub>O<sub>2</sub>.

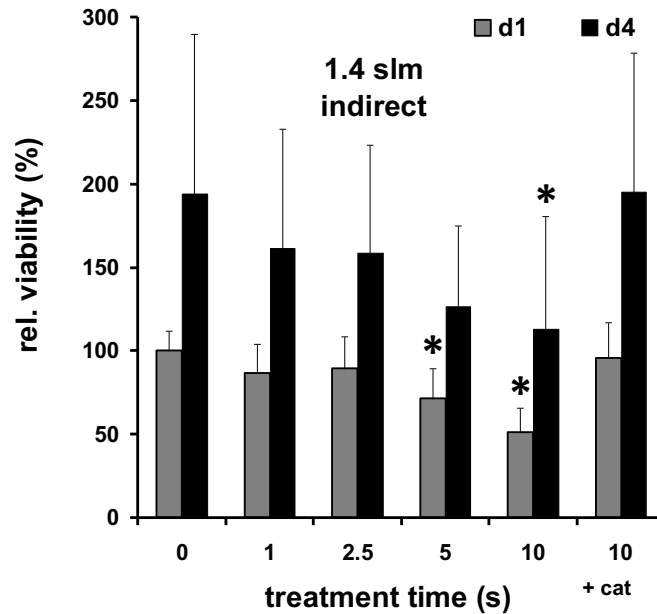


*Fig. XX Proliferation after indirect treatment with 1.40 slm without dilution Assay. Viability of cells on day 1 and 4 after indirect treatment with 1.40 slm plasma for 0, 1, 2.5, 5 and 10 min and an incubation time for 5 min without dilution. In addition, a control with 10 min treated buffer and 5 min incubation time with catalase was given.*

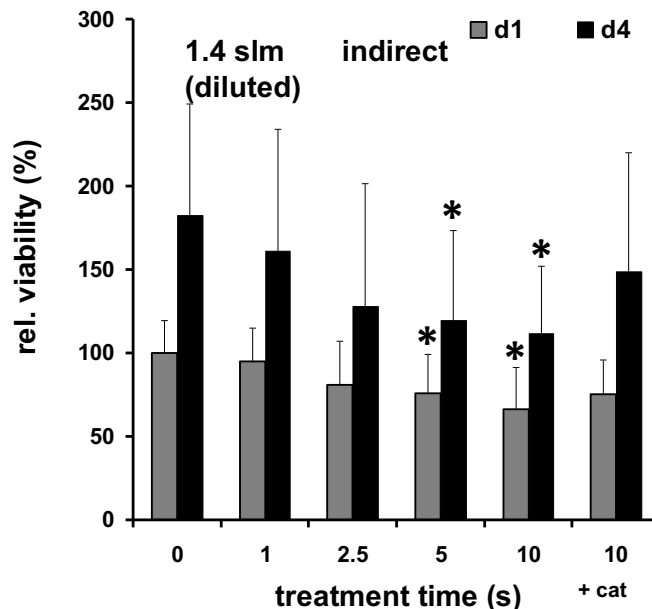


*Fig. XXI Proliferation after indirect treatment with 1.40 slm with dilution Assay. Viability of cells on day 1 and 4 after indirect treatment with 1.40 slm plasma for 0, 1, 2.5, 5 and 10 min and an incubation time for 5 min with compensation with fresh buffer. In addition, a control with 10 min treated buffer and 5 min incubation time with catalase and compensation was given.*

## Results

Using 0.25 slm for plasma generation, indirect and direct treatment (10 min) reduced the cell numbers on day four as compared to the control (see figure XXII, XXIII). The addition of catalase reversed the observed effects induced by indirect treatment. In contrast to the 1.4 slm plasma, the initial cell number on day one was not significantly affected by 0.25 slm plasma treatment.

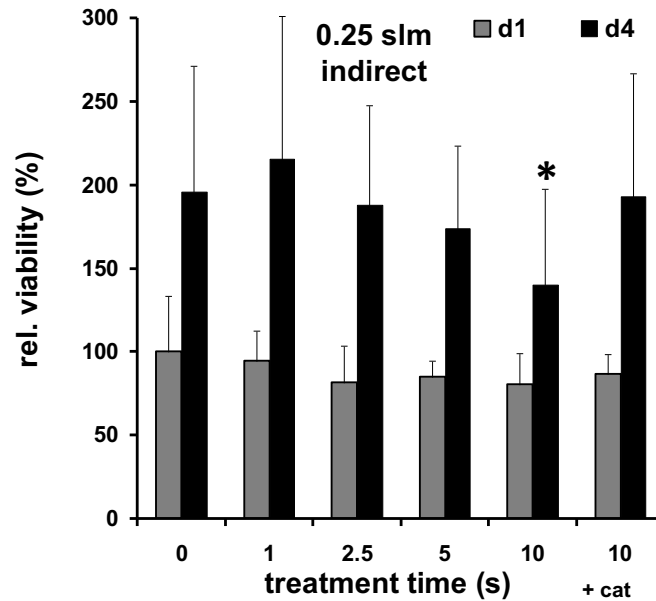


*Fig. XXII Proliferation after indirect treatment with 0.25 slm Assay. Viability of cells on day 1 and 4 after indirect treatment with 0.25 slm plasma for 0, 1, 2.5, 5 and 10 min and an incubation time for 5 min without dilution. In addition, a control with 10 min treated buffer and 5 min incubation time with catalase was given.*

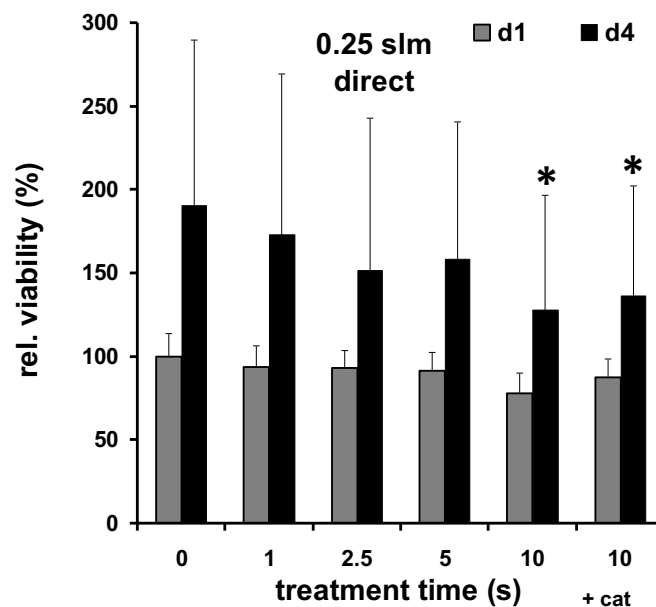


*Fig. XXIII Proliferation after direct treatment with 0.25 slm Assay. Viability of cells on day 1 and 4 after direct treatment with 0.25 slm plasma for 0, 1, 2.5, 5 and 10 min. In addition, a control with 10 min treatment time with catalase was given.*

## Results

Interestingly, the presence of catalase during direct treatment could not reverse the observed antiproliferative effect.

## 4. Discussion

### 4.1 Gas flow of plasma jets without enough buffer medium on cells leads to strong drying-off effects

Investigations of plasma-induced effects bring up some experimental challenges and many studies have used plasma jets and gas flows of 3–6 slm for *in vitro* and *in vivo* experiments. In this regard, small buffer/media volumes were often used for treatment with parallel unknown evaporation rates.

In comparison, our  $\mu$ APPJ could only be operated with a gas flow in the range of 0.25–1.4 slm. On the highest flow rate of 1.4 slm of gas flow, even for one minute, we could not prevent drying-off effects with a buffer layer of 1000  $\mu$ l of PBS (Figure XX). Hence, only indirect treatment with 1.4 slm gas flow were used to avoid falsified cell toxicity due to drying-off-effects and not to plasma treatment. However, it is important to notice that even using a low gas flow of 0.25 slm for 1 minute we could not prevent drying-off effects with a buffer amount of 100 or 250  $\mu$ l on HDFs. At last we could not observe any drying-off effects due to the gas flow with a buffer amount of 500  $\mu$ l. Hence, we only performed direct treatments with that much of buffer on HDFs to gain results due to pure plasma treatment.

This suggest, that we should consider a critical review of studies that operate with plasma jets on living cell types to make sure, that the obtained results are not affected by strong drying-off effects and the pure blow-out of cell medium especially when high flow rates are chosen, which would cause a significant drawback in plasma research.

### 4.2 Treatment with $\mu$ APPJ induces chemical/-physical modifications in buffer

The usage of the  $\mu$ APPJ led to several modifications in the treated buffer. Especially, the comparative amounts of nitrite and nitrate increased. Interestingly, the values obtained after 10 minutes by using a gas flow of 0.25 slm (e.g. Nitrite:

## Discussion

161.4 ± 27.7 μM, Nitrate: 352.7 ± 59.9 μM) were manifold higher than those by using 1.40 slm (e.g. Nitrite: 9.7 ± 2.4 μM, Nitrate: 44.1 ± 6.6 μM). For comparison, the blood plasma of healthy volunteers contained 0.1-0.3 μM nitrite and 14-30 μM nitrate, whereas skin tissue contained 5.1-8.4 μM nitrite and 190-278 μM nitrate [196]. Thus, by applying the μAPPJ on wet biological tissue, an accumulation of nitrite and nitrate could be expected, which may exert biological activity such as increasing the microcirculation in treated area as already shown with DBD devices [197]. In addition, particularly nitrite participates in a number of signaling, for example, in hypoxic signaling events including vasodilation, modulation of mitochondrial respiration, and cytoprotection following ischemic insult [198]. It is also known that acidified nitrite releases NO, strongly enhanced in the presence of antioxidants and metal ions such as Cu<sup>2+</sup> [199]. Moreover, nitrite and acidified nitrite have antimicrobial properties and can inhibit the biofilm formation of *Staphylococcus aureus*, *Staphylococcus epidermidis*, *Pseudomonas aeruginosa*, *Candida albicans* and further human pathogens [200-203]. Thus, plasma-induced acidification and nitrite accumulation may represent an important mechanism to explain the antibacterial effects of plasma [204].

That in turn could benefit wound healing processes e.g. a shortened regeneration time, sterilized wounds (or at least a minimized biofilm) and reduced possibility of developing scar tissue. Additionally, the results in our experiments indicated that the NOD accumulation rate induced by μAPPJ can be regulated by the treatment time and by the gas flow. Hence after optimizing gas flow and buffer on wounds it should be possible to even shorten the necessary treatment time on future patients.

However, plasma/gas treatment in our experimental setting led to an increase in evaporation and a decrease in temperature and concentration of dissolved oxygen in the treated buffer (Figures XI, XIV). The loss of volume by evaporation and the concurrent accumulation of NODs led to hyperosmolarity. Studies showed that this has various effects mammalian cells and tissue, for example, such as inducing cell death in keratinocytes, lymphocytes and endothelial cells [205] or releasing of IL-8 in epithelial cells [206]. In treatment of acute and chronic wounds as well as inflammatory skin diseases this could be a major drawback hence it would lead to an increased inflammatory reaction, a prolonged healing

time and provoke the development of scar tissue. That in turn means it is crucial for future medical applications to optimize the gas flow and the possible addition of nitrogen and/or oxygen to improve the NOD accumulation rate in relation to evaporation, decrease in temperature, concentration of dissolved oxygen to gain the mentioned positive effects in wound healing and preventing scar tissue and avoid the negative outcomes. This could be the main challenge for further investigations in this field.

Furthermore, the presence of  $\text{H}_2\text{O}_2$ , as an oxidant with a disinfectant spectrum and cellular toxicity, has been detected in numerous plasma sources and settings [108, 109]. We investigated whether the  $\mu\text{APPJ}$  was able to produce relevant amounts of  $\text{H}_2\text{O}_2$  in buffer. Here, we found a linear and treatment time-dependent increase of  $\text{H}_2\text{O}_2$  in the treated buffer (Figure XV). Under our experimental conditions, it seemed that plasma induced  $\text{H}_2\text{O}_2$  generation could be at least controlled by gas flow. Many studies had reported the generation/accumulation of  $\text{H}_2\text{O}_2$  in plasma-treated liquids (water, PBS, media) [207]. As described in chapter 4.1 we showed in subsequent control experiments a four-fold reduced concentration of produced  $\text{H}_2\text{O}_2$  by using stainless steel pipes instead of plastic tubes as a gas feed. It is postulated that  $\text{H}_2\text{O}_2$  is generated by a chemical reaction cascade: the OH radical is produced by the photo-dissociation of water by ultraviolet (UV) and vacuum ultraviolet (VUV) radiation and  $\text{H}_2\text{O}_2$  is eventually produced mainly through the  $\text{OH} + \text{OH} \rightarrow \text{H}_2\text{O}_2$  reaction [208]. However, the dissolution of gaseous  $\text{H}_2\text{O}_2$ , produced by gas-plasma reactions, may also play a role in determining the aqueous  $\text{H}_2\text{O}_2$  concentrations, for example, as found in plasma-treated RPMI [209]. Nevertheless, the obtained  $\text{H}_2\text{O}_2$  could have various effects on cells and the microenvironment of wounds.

### 4.3 Treatment with $\mu\text{APPJ}$ reduces cell viability

We evaluated the plasma-induced effects on HDFs as the main cell type of the dermis, which would be most affected by topical treatment of wounds. Thus, the possible effects on the viability were investigated.

## Discussion

In general, we found a moderate toxic effect of plasma on HDFs in our experimental set up. Overall, this toxic effect tended to be correlated with the treatment time. In particular, in indirect plasma treatment, a significant decrease in viability were only obtained after 10 minutes with 1.4 slm and 5 minutes of incubation. After dilution this toxic effect was even weaker. Here, it should be noted, that the final  $\text{H}_2\text{O}_2$  concentration obtained was roughly reduced twofold by this dilution. By addition of catalase to scavenge possible  $\text{H}_2\text{O}_2$  concentrations, the observed reduction of viability could be brought down or totally diminished, indicating the crucial role played by  $\text{H}_2\text{O}_2$  in plasma-induced effects on cells (Figure XVII, XVIII).

The number of cells four days after indirect plasma treatment (1.4 slm, 5 min incubation) was significantly reduced in comparison to the controls. These effects could also be diminished by the addition of catalase for scavenging  $\text{H}_2\text{O}_2$ , which also indicates that plasma induced  $\text{H}_2\text{O}_2$  accumulation was mainly responsible for the reduction of number of cells. However, it seemed that the doubling time of the remaining cells was not different from the control cells, indicating that the lower cell numbers on day four were caused by initial plasma-induced toxic effects. In contrast to a previous study, we could describe these observed effects as antiproliferative effects of short-term incubation with  $\text{H}_2\text{O}_2$  in comparable concentrations (200  $\mu\text{M}$ ) in human foreskin fibroblasts [210].

Also, other studies have shown that short exposures of endothelial cells to hydrogen peroxide with an amount of 50  $\mu\text{M}$  for one hour could induce an elongated inhibition of cell division. An exposure time for two hours and 200  $\mu\text{M}$   $\text{H}_2\text{O}_2$  could also lead fibroblasts F65 to entry a senescence-like state [211]. In our case, the human skin fibroblasts obtained from adults did not show negative effects on proliferation after plasma treatment, although the  $\text{H}_2\text{O}_2$  concentrations obtained were much higher. Therefore, apart from  $\text{H}_2\text{O}_2$  concentration and exposure time, it could be assumed that cell type and cell status are also relevant in judging  $\text{H}_2\text{O}_2$ - and plasma-induced effects in combination to short-time hyperosmolarity.

By using 0.25 slm, the indirect plasma treatment showed a not significant decrease in cell viability. Here, the addition of catalase could not reverse the decreasing effect of 0.25 slm plasma on cell viability, which indicates that the

higher amounts of nitrite/nitrate obtained in this case may be involved, as shown in a previous study [212].

Using 0.25 slm for plasma generation, direct and indirect treatment (10 min) reduced the cell numbers on day four as compared to the control. The addition of catalase reversed the observed effects induced by indirect treatment. In contrast to the 1.4 slm plasma, the initial cell number on day one was not significantly affected by 0.25 slm plasma treatment. Therefore, it may be assumed that the low gas flow plasma induced an antiproliferative effect with low toxicity. Interestingly, the presence of catalase during direct treatment could not reverse the observed antiproliferative effect, indicating the existence of further mechanisms. These effects may be partially mediated by UV radiation besides  $H_2O_2$  and possibly by higher concentration of nitrogen species, such as nitrite, which may react with  $H_2O_2$  to form other species (peroxynitrite) and/or a direct inactivation of the catalase by direct exposure to the plasma.

Although toxicity was generally low, our results demonstrated a delayed toxicity, which seemed to be dependent on  $H_2O_2$  or nitrite/nitrate concentrations and exposure time. With regard to limited perfusion in the wound area, plasma-treated wound fluid will be diluted or replaced slowly; therefore, the retention time of plasma-induced bioactive species, such as  $H_2O_2$  and nitrite, could also have a significant influence on the biological outcome and thus needs further investigations.

### 4.4 Chances of the $\mu$ APPJ in clinical usage for treatments of wounds and other tissues

Hence the CAP produced by the  $\mu$ APPJ operated with helium gas led to just low cell toxicity and exerted remarkable amounts of NOD and  $H_2O_2$  that were presumably relevant for the described effects on HDFs, a treatment of patients with  $\mu$ APPJ in the future could be possible but needs further investigations. A promising approach would be the treatment of scaphoids, wounds which healing process would approximately lead to scar tissue (e.g. infected wounds, wounds due to severe burning) or wounds where scar tissue development should

## Discussion

definitely be avoided (wounds near joints, face wounds). In these cases, the observed cell toxicity (especially after longer treatment time of 10 min) in combination to the nitrate/nitrite and  $H_2O_2$  accumulation that lead to vasodilatation as well as the described sterilizing effects [213] could be exploited to diminish scaphoid development prior manifestation or treat already emerged scar tissue. Hence, it could be a possible aesthetic as well as medical treatment of wounds and scars without any operation. Studies showed that early gestational fetal skin partly undergoes a scarless wound healing regarding to a lack of an inflammation phase [56]. Hence the CAP treatment could induce an elevated concentration of  $H_2O_2$  in the microenvironment, probably the inflammation phase in wound healing may be partly suppressed as seen in other studies, where the appropriate level of hydrogen peroxide results in an increased expression of transforming growth factor-1, enhanced proliferation of fibroblasts and collagen deposition, resulting in an improved wound healing following a scarless tissue transformation [57, 214].

But to gain a positive outcome of CAP treatment it is crucial to optimize the gas flow relating to the treated tissue to avoid severe evaporation and hyperosmolarity resulting in impaired wound healing and promoting scar tissue instead of shortened healing time, pleasant appearance and functional integrity (see figure XXIV).

## Discussion

In comparison to CAP sources that produce plasma with a gas flow of 6 slm, the opportunity to operate at very low gas flows, such as 0.25 slm, and make small adjustments the COST reference microplasma jet could be used to do further investigations to find the best possible treatment flow due to the treated surface.

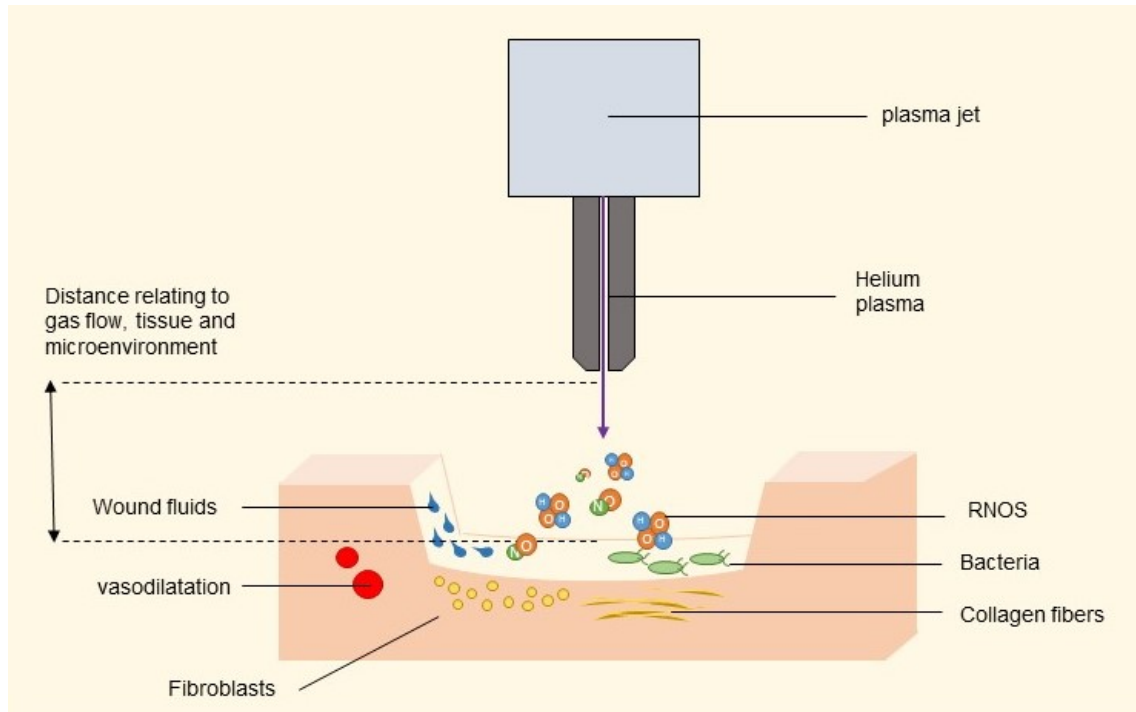


**Fig. XXIV Plasma Jet schematically treating wounds.** Through treatment NOD an  $H_2O_2$  accumulates in the wound and lead to significant osmolarity changes and cause vasodilatation, sterilization, low cell toxicity without drying of effects. The wound fluids functions as buffer medium an was constantly replaced by secretion. The distance of the CAP source had to be individual defined due to gas flow, kind of tissue and amount wound fluid.

Regarding to the need to individual define the distance and flow of the COST reference microplasma jet before every treatment it could be very challenging to find a composition that can be used anywhere and limit the clinical usage of this device. The key to an everyday usage is firstly a smaller size of the jet, in best case a handy device, secondly an easier way to treat different tissues without measuring the distance up to millimeters, and thirdly that the patient must hold completely still during treatment time.

In comparison to other plasma sources, for example the hybrid plasma sources, where micro discharges happen parallel to the surface of a dielectric barrier, where no air gap is between barrier and counter electrode. These devices could be much more practical in an everyday usage in clinics that also can be used by untrained medical professionals.

## 4.5 Ambient atmosphere and system's gas tubing could affect the plasma characterization and biological effects

As shown in the optical emission spectroscopy other lines apart from the expected operating gases (helium and oxygen) were detected, indicating that besides stable experiment conditions the device itself and the ambient atmosphere could lead to different compounds of the generated plasma. These other atoms and molecules could be attributed to backflow from ambient atmosphere. In addition, we found a marked peak at 308 nm that indicated the presence of OH in the plasma phase. This presence may be attributed to the stored humidity in the system's gas tubing. Since the  $\mu$ APPJ was operated with helium, traces of water in the delivery system could produce these peaks. Therefore, the observed  $\text{H}_2\text{O}_2$  accumulation in the treated buffer could also be attributed to these impurities.

Establishing a reference jet based on  $\mu$ APPJ - the COST jet – Schulz von der Gathen and co-workers could show the importance of, for example, the material of the gas lines on the purity and reproducibility of the generated plasma [215, 216]. Indeed, we showed in subsequent control experiments that used stainless steel pipes instead of plastic pipes different OES spectra were obtained. Therefore, water contamination was reduced, resulting in a reduction of OH peak (OES) and also a four-fold reduction of the accumulated concentrations of  $\text{H}_2\text{O}_2$  when a gas flow of 1.40 slm was used (see supplement figures I and II).

Consequently, our results showed the high sensitivity of a plasma source or the generated CAP to small interfering factors. However, apart from the gas flow, the defined addition, e.g., of oxygen and/or water may modified the plasma's characteristics and plasma-induced biological effects, which in turn could be exploited for the treatment of contaminated surfaces and biological tissues. Hence, the transition from *in vitro* to *in vivo* usage of indirect plasma sources as the COST reference microplasma jet needs much more research, not just in more experiments of using the COST reference microplasma jet, the jet itself has to be developed to gain a significant importance in future applications and a possible everyday usage in clinics. At this moment, regarding the promising effects of wound healing and preventing development of scar tissue, the next steps in future

## Discussion

investigations should be the treatment of human or animal skin tissue to see the CAP effect on tissue and not just the effects on artificial buffer and cultured cells, encouraging the research to *in vivo* treatment of infectious or scaphoid wounds.

## 5. Conclusion

Cold atmospheric-pressure plasmas exert biochemical effects, cellular toxicity, which are mainly based on the accumulation nitrogen species and reactive oxygen during treatment. However, cell survival depends on a wet environment with a stable physiological pH, osmolarity, temperature as well as an adequate supply of oxygen and nutrient. Plasma jets in particular interfere with the osmolarity, oxygen concentration and temperature of the cellular microenvironment by using relatively high gas flows (up to 6 slm). In this study, we have used  $\mu$ APPJ as the CAP source, which could be operated with lower gas flows to avoid excessive changes and dry out effects. Our results indicated that under our experimental conditions, cell viability and proliferation are only weakly influenced by short term increase of osmolarity and decrease of oxygen induced by the gas flow alone. However, the gas flow had a strong impact on CAP-induced effects on liquids, which in turn resulted in different biological responses. In our case, the accumulation of  $H_2O_2$  and NOD within the buffer could be influenced and controlled, which could be beneficial for medical treatments. Our results also showed the generated CAP to be highly sensitivity to small interfering factors such as impurities, which may hamper the comparability of studies. Nevertheless, via the defined addition of oxygen, nitrogen and water, the plasma characteristics and plasma-induced biological effects could be modulated, which in turn may be beneficial for the medical use of the  $\mu$ APPJ as a CAP source.

In general, the  $\mu$ APPJ exerted low toxicity on cells and only longer treatment time influenced cell viability and potential proliferation. Regarding the potential sterilizing effects of the generated plasma effluent, the  $\mu$ APPJ seemed to be suitable for the treatment of contaminated dermal wounds and other tissues. Therefore, further studies are necessary to maximize the beneficial antibacterial and wound healing-promoting effects of plasma treatment and to minimize hazardous effects, which may result, for example, in impaired wound healing. On the other hand, the observed reduced cell viability after CAP treatment may lead to a new approach in treatment of scaphoids that need further investigations.

## 6. References

1. Rassner, G., *Dermatologie*. 2009: Elsevier Urban & Fischer Verlag. p. 5-9.
2. Metelmann, H.v.W., T.; Weltmann, K., *Plasmamedizin: Kaltplasma in der medizinischen Anwendung*. 2016, Springer Verlag. p. 4-14.
3. Kröncke, K.-D., C.V. Suschek, and V. Kolb-Bachofen, *Implications of Inducible Nitric Oxide Synthase Expression and Enzyme Activity*. *Antioxidants & Redox Signaling*, 2000. **2**(3): p. 585-605.
4. Hirner, A. and K. Weise, *Chirurgie*. 2004: Thieme Verlag. p. 32-34.
5. Schumpelick, V., N. Bleese, and U. Mommsen, *Kurzlehrbuch Chirurgie*. 2006: Thieme Verlag. p. 25-34.
6. Sterry, W., *Kurzlehrbuch Dermatologie*. 2011: Thieme Verlag. p. 3-7.
7. Netter, F.H., *Netters Dermatologie*. 2010: Thieme Verlag.
8. Schmidt, A., et al., *Non-thermal plasma activates human keratinocytes by stimulation of antioxidant and phase II pathways*. *J Biol Chem*, 2015. **290**(11): p. 6731-50.
9. Tracy, L.E., R.A. Minasian, and E.J. Caterson, *Extracellular Matrix and Dermal Fibroblast Function in the Healing Wound*. *Adv Wound Care (New Rochelle)*, 2016. **5**(3): p. 119-136.
10. Sorrell, J.M., M.A. Baber, and A.I. Caplan, *Site-matched papillary and reticular human dermal fibroblasts differ in their release of specific growth factors/cytokines and in their interaction with keratinocytes*. *J Cell Physiol*, 2004. **200**(1): p. 134-45.
11. Sorrell, J.M. and A.I. Caplan, *Fibroblast heterogeneity: more than skin deep*. *J Cell Sci*, 2004. **117**(Pt 5): p. 667-75.
12. Sorrell, J.M., M.A. Baber, and A.I. Caplan, *Clonal characterization of fibroblasts in the superficial layer of the adult human dermis*. *Cell Tissue Res*, 2007. **327**(3): p. 499-510.
13. Nolte, S.V., et al., *Diversity of fibroblasts--a review on implications for skin tissue engineering*. *Cells Tissues Organs*, 2008. **187**(3): p. 165-76.
14. Welsch, U. and T. Deller, *Lehrbuch Histologie*. 2010, Elsevier Verlag Urban & Fischer. p. 92-94.
15. Donovan, J., D. Abraham, and J. Norman, *Platelet-derived growth factor signaling in mesenchymal cells*. *Front Biosci (Landmark Ed)*, 2013. **18**: p. 106-19.
16. Sakai, S., et al., *In vivo evaluation of human skin anisotropy by polarization-sensitive optical coherence tomography*. *Biomed Opt Express*, 2011. **2**(9): p. 2623-31.
17. Junker, J.P., et al., *Mechanical tension stimulates the transdifferentiation of fibroblasts into myofibroblasts in human burn scars*. *Burns*, 2008. **34**(7): p. 942-6.
18. Kraissl, C.J., *The selection of appropriate lines for elective surgical incisions*. *Plast Reconstr Surg (1946)*, 1951. **8**(1): p. 1-28.
19. Baur, P.S., D.L. Larson, and T.R. Stacey, *The observation of myofibroblasts in hypertrophic scars*. *Surg Gynecol Obstet*, 1975. **141**(1): p. 22-6.
20. Liu, F., et al., *Feedback amplification of fibrosis through matrix stiffening and COX-2 suppression*. *J Cell Biol*, 2010. **190**(4): p. 693-706.
21. Prager-Khoutorsky, M., et al., *Fibroblast polarization is a matrix-rigidity-dependent process controlled by focal adhesion mechanosensing*. *Nat Cell Biol*, 2011. **13**(12): p. 1457-65.
22. Huang, X., et al., *Matrix stiffness-induced myofibroblast differentiation is mediated by intrinsic mechanotransduction*. *Am J Respir Cell Mol Biol*, 2012. **47**(3): p. 340-8.
23. Marinkovic, A., et al., *Improved throughput traction microscopy reveals pivotal role for matrix stiffness in fibroblast contractility and TGF-beta responsiveness*. *Am J Physiol Lung Cell Mol Physiol*, 2012. **303**(3): p. L169-80.

## References

24. Leight, J.L., et al., *Matrix rigidity regulates a switch between TGF-beta1-induced apoptosis and epithelial-mesenchymal transition*. Mol Biol Cell, 2012. **23**(5): p. 781-91.
25. Karamichos, D., R.A. Brown, and V. Mudera, *Collagen stiffness regulates cellular contraction and matrix remodeling gene expression*. J Biomed Mater Res A, 2007. **83**(3): p. 887-94.
26. Derderian, C.A., et al., *Mechanical strain alters gene expression in an in vitro model of hypertrophic scarring*. Ann Plast Surg, 2005. **55**(1): p. 69-75; discussion 75.
27. Langmuir, I., *The Interaction of Electron and Positive Ion Space Charges in Cathode Sheaths*. Physical Review, 1929. **33**(6): p. 954-989.
28. Nosenko, T., T. Shimizu, and G.E. Morfill, *Designing plasmas for chronic wound disinfection*. New Journal of Physics, 2009. **11**(11): p. 115013.
29. Heinlin, J., et al., *Plasma medicine: possible applications in dermatology*. J Dtsch Dermatol Ges, 2010. **8**(12): p. 968-76.
30. U., S., *Plasmaphysik: Phänomene, Grundlagen, Anwendungen*. 2011: Springer Verlag. p. 1-3.
31. Bittencourt, J.A., *Fundamentals of Plasma Physics*. 2004: Springer Verlag. 1-4.
32. Tendero, C., et al., *Atmospheric pressure plasmas: A review*. Spectrochimica Acta Part B: Atomic Spectroscopy, 2006. **61**(1): p. 2-30.
33. Lee, H.J., et al., *Degradation of adhesion molecules of G361 melanoma cells by a non-thermal atmospheric pressure microplasma*. New Journal of Physics, 2009. **11**(11): p. 115026.
34. Park, G.Y., et al., *Atmospheric-pressure plasma sources for biomedical applications*. Plasma Sources Science and Technology, 2012. **21**(4): p. 043001.
35. d'Agostino, R., et al., *Low-Temperature Plasma Processing of Materials: Past, Present, and Future*. Plasma Processes and Polymers, 2005. **2**(1): p. 7-15.
36. Hauser, J., et al., *[Surface modification of metal implant materials by low-pressure plasma treatment]*. Biomed Tech (Berl), 2009. **54**(2): p. 98-106.
37. Laroussi, M., *Sterilization of contaminated matter with an atmospheric pressure plasma*. IEEE Transactions on Plasma Science, 1996. **24**(3): p. 1188-1191.
38. Kong, M.G., et al., *Plasma medicine: an introductory review*. New Journal of Physics, 2009. **11**(11): p. 115012.
39. Sladek, R.E.J. and E. Stoffels, *Deactivation of Escherichia coli by the plasma needle*. Journal of Physics D: Applied Physics, 2005. **38**(11): p. 1716.
40. Basaran, P., N. Basaran-Akgul, and L. Oksuz, *Elimination of Aspergillus parasiticus from nut surface with low pressure cold plasma (LPCP) treatment*. Food Microbiology, 2008. **25**(4): p. 626-632.
41. Terrier, O., et al., *Cold oxygen plasma technology efficiency against different airborne respiratory viruses*. Journal of Clinical Virology, 2009. **45**(2): p. 119-124.
42. Laroussi, M., D.A. Mendis, and M. Rosenberg, *Plasma interaction with microbes*. New Journal of Physics, 2003. **5**(1): p. 41.
43. Laroussi, M., *Nonthermal decontamination of biological media by atmospheric-pressure plasmas: review, analysis, and prospects*. IEEE Transactions on Plasma Science, 2002. **30**(4): p. 1409-1415.
44. Alexeff, I., et al. *Atmospheric Pressure Resistive Barrier Cold Plasma for Biological Decontamination*. in *IEEE Conference Record - Abstracts. 2005 IEEE International Conference on Plasma Science*. 2005.
45. Sladek, R.E., et al., *Treatment of Streptococcus mutans biofilms with a nonthermal atmospheric plasma*. Lett Appl Microbiol, 2007. **45**(3): p. 318-23.
46. Venezia, R.A., et al., *Lethal activity of nonthermal plasma sterilization against microorganisms*. Infect Control Hosp Epidemiol, 2008. **29**(5): p. 430-6.

## References

47. Kamgang-Youbi, G., et al., *Microbial inactivation using plasma-activated water obtained by gliding electric discharges*. Letters in Applied Microbiology, 2009. **48**(1): p. 13-18.
48. Hee Lee, M., et al., *Removal and sterilization of biofilms and planktonic bacteria by microwave-induced argon plasma at atmospheric pressure*. New Journal of Physics, 2009. **11**(11): p. 115022.
49. Deng, X.T., J.J. Shi, and M.G. Kong, *Protein destruction by a helium atmospheric pressure glow discharge: Capability and mechanisms*. Journal of Applied Physics, 2007. **101**(7): p. 074701.
50. Daeschlein, G., et al., *In Vitro Susceptibility of Important Skin and Wound Pathogens Against Low Temperature Atmospheric Pressure Plasma Jet (APPJ) and Dielectric Barrier Discharge Plasma (DBD)*. Plasma Processes and Polymers, 2012. **9**(4): p. 380-389.
51. Daeschlein, G., et al., *In Vitro Susceptibility of Multidrug Resistant Skin and Wound Pathogens Against Low Temperature Atmospheric Pressure Plasma Jet (APPJ) and Dielectric Barrier Discharge Plasma (DBD)*. Plasma Processes and Polymers, 2014. **11**(2): p. 175-183.
52. Zhang, X., et al., *Ablation of liver cancer cells in vitro by a plasma needle*. Applied Physics Letters, 2008. **93**(2): p. 021502.
53. Ginsberg, G.G., et al., *The argon plasma coagulator: February 2002*. Gastrointest Endosc, 2002. **55**(7): p. 807-10.
54. Morrison, J.C.F., *Electrosurgical method and apparatus for initiating an electrical discharge in an inert gas flow*. 1977: US.
55. Arndt, S., et al., *Cold atmospheric plasma, a new strategy to induce senescence in melanoma cells*. Exp Dermatol, 2013. **22**(4): p. 284-9.
56. Ahn, H.J., et al., *Targeting Cancer Cells with Reactive Oxygen and Nitrogen Species Generated by Atmospheric-Pressure Air Plasma*. PLOS ONE, 2014. **9**(1): p. e86173.
57. Kang, S.U., et al., *Nonthermal plasma induces head and neck cancer cell death: the potential involvement of mitogen-activated protein kinase-dependent mitochondrial reactive oxygen species*. Cell Death Dis, 2014. **5**: p. e1056.
58. Fridman, G., et al., *Floating Electrode Dielectric Barrier Discharge Plasma in Air Promoting Apoptotic Behavior in Melanoma Skin Cancer Cell Lines*. Plasma Chemistry and Plasma Processing, 2007. **27**(2): p. 163-176.
59. Kim, J.Y., et al., *Apoptosis of lung carcinoma cells induced by a flexible optical fiber-based cold microplasma*. Biosens Bioelectron, 2011. **28**(1): p. 333-8.
60. Lee, S.Y., et al., *Nonthermal plasma induces apoptosis in ATC cells: involvement of JNK and p38 MAPK-dependent ROS*. Yonsei Med J, 2014. **55**(6): p. 1640-7.
61. Panngom, K., et al., *Preferential killing of human lung cancer cell lines with mitochondrial dysfunction by nonthermal dielectric barrier discharge plasma*. Cell Death Dis, 2013. **4**: p. e642.
62. Yan, X., et al., *Plasma-Induced Death of HepG2 Cancer Cells: Intracellular Effects of Reactive Species*. Plasma Processes and Polymers, 2012. **9**(1): p. 59-66.
63. Bogle, M.A., K.A. Arndt, and J.S. Dover, *Evaluation of plasma skin regeneration technology in low-energy full-facial rejuvenation*. Arch Dermatol, 2007. **143**(2): p. 168-74.
64. Fitzpatrick, R., et al., *A histopathologic evaluation of the Plasma Skin Regeneration System (PSR) versus a standard carbon dioxide resurfacing laser in an animal model*. Lasers Surg Med, 2008. **40**(2): p. 93-9.
65. Foster, K.W., R.L. Moy, and E.F. Fincher, *Advances in plasma skin regeneration*. J Cosmet Dermatol, 2008. **7**(3): p. 169-79.
66. Kilmer, S., et al., *Long term follow-up on the use of plasma skin regeneration (PSR) in full facial rejuvenation procedures*. Lasers in Surgery and Medicine, 2005: p. 8-8.

## References

67. Wang, J., et al., *Tooth Enamel Evaluation After Tooth Bleaching With Hydrogen Peroxide Assisted by a DC Nonthermal Atmospheric-Pressure Plasma Jet*. IEEE Transactions on Plasma Science, 2012. **40**(9): p. 2157-2162.
68. Lee, H.W., et al., *Tooth bleaching with nonthermal atmospheric pressure plasma*. J Endod, 2009. **35**(4): p. 587-91.
69. Robson, M.C. and J.P. Heggors, *Delayed wound closure based on bacterial counts*. J Surg Oncol, 1970. **2**(4): p. 379-83.
70. Kalghatgi, S., et al. *Non-thermal plasma treatment enhances proliferation of endothelial cells*. in *Second International Conference on Plasma Medicine*. San Antonio, Texas, USA. 2009.
71. Trengove, N.J., et al., *Qualitative bacteriology and leg ulcer healing*. J Wound Care, 1996. **5**(6): p. 277-80.
72. Haertel, B., et al., *Non-thermal atmospheric-pressure plasma possible application in wound healing*. Biomolecules & therapeutics, 2014. **22**(6): p. 477-490.
73. Shekhter, A.B., et al., *Experimental and clinical validation of plasmadynamic therapy of wounds with nitric oxide*. Bulletin of Experimental Biology and Medicine, 1998. **126**(2): p. 829-834.
74. Lipatov, K.V., et al., *[Use of gas flow with nitrogen oxide (NO-therapy) in combined treatment of purulent wounds]*. Khirurgiia (Mosk), 2002(2): p. 41-3.
75. Fridman, G., et al., *Applied Plasma Medicine*. Plasma Processes and Polymers, 2008. **5**(6): p. 503-533.
76. Fridman, G.B., A.D.; Balasubramanian, M.; Fridman, A.; Gutsol, A.; Vasilets, V.N.; Ayan, H.; Friedman, G., *Comparison of Direct and Indirect Effects of Non-Thermal Atmospheric-Pressure Plasma on Bacteria*. Plasma Process Polym, 2007. **4**: **370-5**.
77. Shimizu, T., et al., *Characterization of Microwave Plasma Torch for Decontamination*. Plasma Processes and Polymers, 2008. **5**(6): p. 577-582.
78. Cao, Z., J.L. Walsh, and M.G. Kong, *Atmospheric plasma jet array in parallel electric and gas flow fields for three-dimensional surface treatment*. Applied Physics Letters, 2009. **94**(2): p. 021501.
79. Morfill, G.E., et al., *Nosocomial infections—a new approach towards preventive medicine using plasmas*. New Journal of Physics, 2009. **11**(11): p. 115019.
80. Lademann, J., et al., *Risk assessment of the application of a plasma jet in dermatology*. J Biomed Opt, 2009. **14**(5): p. 054025.
81. Karl, H.S., et al., *High-pressure hollow cathode discharges*. Plasma Sources Science and Technology, 1997. **6**(4): p. 468.
82. Eden, J.G., et al., *Microplasma devices fabricated in silicon, ceramic, and metal/polymer structures: arrays, emitters and photodetectors*. Journal of Physics D: Applied Physics, 2003. **36**(23): p. 2869.
83. Baars-Hibbe, L., et al., *High frequency glow discharges at atmospheric pressure with micro-structured electrode arrays*. Journal of Physics D: Applied Physics, 2005. **38**(4): p. 510.
84. Torben, H., et al., *Spatially resolved simulation of a radio-frequency driven micro-atmospheric pressure plasma jet and its effluent*. Journal of Physics D: Applied Physics, 2011. **44**(28): p. 285206.
85. McKay, K., et al., *Dynamics and particle fluxes in atmospheric-pressure electronegative radio frequency microplasmas*. Applied Physics Letters, 2011. **99**(9): p. 091501.
86. Niemi, K., et al., *Diagnostic based modeling for determining absolute atomic oxygen densities in atmospheric pressure helium-oxygen plasmas*. Applied Physics Letters, 2009. **95**(15): p. 151504.
87. Niemi, K., et al., *The role of helium metastable states in radio-frequency driven helium–oxygen atmospheric pressure plasma jets: measurement and numerical simulation*. Plasma Sources Science and Technology, 2011. **20**(5): p. 055005.

## References

88. Shi, J.J. and M.G. Kong, *Mechanisms of the  $\alpha$  and  $\gamma$  modes in radio-frequency atmospheric glow discharges*. Journal of Applied Physics, 2005. **97**(2): p. 023306.
89. Yang, A., et al., *1-D fluid model of atmospheric-pressure rf He+O<sub>2</sub> cold plasmas: Parametric study and critical evaluation*. Physics of Plasmas, 2011. **18**(11): p. 113503.
90. Ellerweg, D., et al., *Characterization of the effluent of a He/O<sub>2</sub> microscale atmospheric pressure plasma jet by quantitative molecular beam mass spectrometry*. New Journal of Physics, 2010. **12**(1): p. 013021.
91. Herrmann, H.W., et al., *Decontamination of chemical and biological warfare (CBW) agents using an atmospheric pressure plasma jet (APPJ)*. Physics of Plasmas, 1999. **6**(5): p. 2284-2289.
92. Gibson, A.R., et al., *Interactions of a Non-Thermal Atmospheric Pressure Plasma Effluent with PC-3 Prostate Cancer Cells*. Plasma Processes and Polymers, 2014. **11**(12): p. 1142-1149.
93. O'Connell, D., et al., *Cold atmospheric pressure plasma jet interactions with plasmid DNA*. Applied Physics Letters, 2011. **98**(4): p. 043701.
94. Coulombe, S., et al., *Miniature atmospheric pressure glow discharge torch (APGD-t) for local biomedical applications*. Pure and Applied Chemistry, 2006. **78**(6).
95. Foest, R., et al., *RF Capillary Jet - a Tool for Localized Surface Treatment*. Contributions to plasma physics, 2007. **47**(1-2): p. 119-128.
96. Voráč, J., et al., *Measurement of hydroxyl radical (OH) concentration in an argon RF plasma jet by laser-induced fluorescence*. Plasma Sources Science and Technology, 2013. **22**(2): p. 025016.
97. Robert, E., et al., *Experimental Study of a Compact Nanosecond Plasma Gun*. Plasma Processes and Polymers, 2009. **6**(12): p. 795-802.
98. Ehlbeck, J., et al., *Low temperature atmospheric pressure plasma sources for microbial decontamination*. Journal of Physics D: Applied Physics, 2011. **44**(1): p. 013002.
99. Von Woedtke, T.M., M.R.; Weltmann, K.D., *Clinical Plasma Medicine: State and Perspectives of in Vivo Application of Cold Atmospheric Plasma*. Contributions to plasma physics, 2014. **54**(2): **104-17**.
100. Liebmann, J., et al., *Biological effects of nitric oxide generated by an atmospheric pressure gas-plasma on human skin cells*. Nitric Oxide, 2011. **24**(1): p. 8-16.
101. Kalghatgi, S., et al., *Endothelial cell proliferation is enhanced by low dose non-thermal plasma through fibroblast growth factor-2 release*. Ann Biomed Eng, 2010. **38**(3): p. 748-57.
102. Haertel, B., et al., *Surface molecules on HaCaT keratinocytes after interaction with non-thermal atmospheric pressure plasma*. Cell Biology International, 2012. **36**(12): p. 1217-1222.
103. Haertel, B., et al., *Differential influence of components resulting from atmospheric-pressure plasma on integrin expression of human HaCaT keratinocytes*. Biomed Res Int, 2013. **2013**: p. 761451.
104. Shi, X.-M., et al., *Effects of Low-Temperature Atmospheric Air Plasmas on the Activity and Function of Human Lymphocytes*. Plasma Processes and Polymers, 2008. **5**(5): p. 482-488.
105. Haertel, B., et al., *Differential sensitivity of lymphocyte subpopulations to non-thermal atmospheric-pressure plasma*. Immunobiology, 2012. **217**(6): p. 628-33.
106. Oehmigen, K., et al., *The Role of Acidification for Antimicrobial Activity of Atmospheric Pressure Plasma in Liquids*. Plasma Processes and Polymers, 2010. **7**(3-4): p. 250-257.
107. Arjunan, K.P., et al., *Non-thermal dielectric barrier discharge plasma induces angiogenesis through reactive oxygen species*. J R Soc Interface, 2012. **9**(66): p. 147-57.
108. Bekeschus, S., et al., *Hydrogen peroxide: A central player in physical plasma-induced oxidative stress in human blood cells*. Free Radic Res, 2014. **48**(5): p. 542-9.

## References

109. Chuin, C.L., et al., *Mass Spectrometric Detection of Gaseous Hydrogen Peroxide in Ambient Air Using Dielectric Barrier Discharge as an Excitation Source*. Chemistry Letters, 2009. **38**(6): p. 520-521.
110. Lancaster, J.R., Jr., *A tutorial on the diffusibility and reactivity of free nitric oxide*. Nitric Oxide, 1997. **1**(1): p. 18-30.
111. Schmidt, K., et al., *Release of nitric oxide from donors with known half-life: a mathematical model for calculating nitric oxide concentrations in aerobic solutions*. Naunyn Schmiedebergs Arch Pharmacol, 1997. **355**(4): p. 457-62.
112. McGrath, H., Jr., *Ultraviolet-A1 irradiation decreases clinical disease activity and autoantibodies in patients with systemic lupus erythematosus*. Clin Exp Rheumatol, 1994. **12**(2): p. 129-35.
113. Feelisch, M., [*Nitrogen monoxide (NO)--the active principle of organic nitrates*]. Schweiz Rundsch Med Prax, 1993. **82**(42): p. 1167-71.
114. Doran, T.I., A. Vidrich, and T.T. Sun, *Intrinsic and extrinsic regulation of the differentiation of skin, corneal and esophageal epithelial cells*. Cell, 1980. **22**(1 Pt 1): p. 17-25.
115. Bredt, D.S., et al., *Cloned and expressed nitric oxide synthase structurally resembles cytochrome P-450 reductase*. Nature, 1991. **351**(6329): p. 714-8.
116. Alderton, W.K., C.E. Cooper, and R.G. Knowles, *Nitric oxide synthases: structure, function and inhibition*. Biochemical Journal, 2001. **357**(Pt 3): p. 593-615.
117. Bredt, D.S., P.M. Hwang, and S.H. Snyder, *Localization of nitric oxide synthase indicating a neural role for nitric oxide*. Nature, 1990. **347**(6295): p. 768-70.
118. Mayer, B., M. John, and E. Böhme, *Purification of a Ca<sup>2+</sup>/calmodulin-dependent nitric oxide synthase from porcine cerebellum: Cofactor-role of tetrahydrobiopterin*. FEBS Letters, 1990. **277**(1-2): p. 215-219.
119. Knowles, R.G. and S. Moncada, *Nitric oxide synthases in mammals*. Biochem J, 1994. **298** ( Pt 2): p. 249-58.
120. Moncada, S. and E.A. Higgs, *Endogenous nitric oxide: physiology, pathology and clinical relevance*. Eur J Clin Invest, 1991. **21**(4): p. 361-74.
121. Nathan, C. and Q.W. Xie, *Nitric oxide synthases: roles, tolls, and controls*. Cell, 1994. **78**(6): p. 915-8.
122. Ruan, J., et al., *Inducible Nitric Oxide Synthase Requires Both the Canonical Calmodulin-binding Domain and Additional Sequences in Order to Bind Calmodulin and Produce Nitric Oxide in the Absence of Free Ca<sup>2+</sup>*. Journal of Biological Chemistry, 1996. **271**(37): p. 22679-22686.
123. Jurkiewicz, B.A. and G.R. Buettner, *Ultraviolet light-induced free radical formation in skin: an electron paramagnetic resonance study*. Photochem Photobiol, 1994. **59**(1): p. 1-4.
124. Laurent, M., M. Lepoivre, and J.P. Tenu, *Kinetic modelling of the nitric oxide gradient generated in vitro by adherent cells expressing inducible nitric oxide synthase*. Biochem J, 1996. **314** ( Pt 1): p. 109-13.
125. Suschek, C.V., et al., *Nitrite, a naturally occurring precursor of nitric oxide that acts like a 'prodrug'*. Biol Chem, 2006. **387**(5): p. 499-506.
126. Dejam, A., et al., *Thiols enhance NO formation from nitrate photolysis*. Free Radic Biol Med, 2003. **35**(12): p. 1551-9.
127. Granger, D.L., et al., *Metabolic fate of L-arginine in relation to microbiostatic capability of murine macrophages*. J Clin Invest, 1990. **85**(1): p. 264-73.
128. Stuehr, D.J.N., C.F., *Nitric oxide. A macrophage product responsible for cytostasis and respiratory inhibition in tumor target cells*. The Journal of Experimental Medicine, 1989. **169**(5): p. 1543-1555.
129. Liew, F.Y. and F.E. Cox, *Nonspecific defence mechanism: the role of nitric oxide*. Immunol Today, 1991. **12**(3): p. A17-21.

## References

130. Rachmilewitz, D., et al., *Enhanced colonic nitric oxide generation and nitric oxide synthase activity in ulcerative colitis and Crohn's disease*. Gut, 1995. **36**(5): p. 718-23.
131. Kooy, N.W., et al., *Extensive tyrosine nitration in human myocardial inflammation: evidence for the presence of peroxynitrite*. Crit Care Med, 1997. **25**(5): p. 812-9.
132. Bruch-Gerharz, D., et al., *Arginase 1 overexpression in psoriasis: limitation of inducible nitric oxide synthase activity as a molecular mechanism for keratinocyte hyperproliferation*. Am J Pathol, 2003. **162**(1): p. 203-11.
133. Seabra, A.B., et al., *S-nitrosoglutathione-containing hydrogel increases dermal blood flow in streptozotocin-induced diabetic rats*. British Journal of Dermatology, 2007. **156**(5): p. 814-818.
134. Lee, P.C., et al., *Impaired wound healing and angiogenesis in eNOS-deficient mice*. Am J Physiol, 1999. **277**(4 Pt 2): p. H1600-8.
135. Joshi, M., J. Strandhoy, and W.L. White, *Nitric oxide synthase activity is up-regulated in melanoma cell lines: a potential mechanism for metastases formation*. Melanoma Res, 1996. **6**(2): p. 121-6.
136. Wink, D.A., et al., *DNA deaminating ability and genotoxicity of nitric oxide and its progenitors*. Science, 1991. **254**(5034): p. 1001-3.
137. Kroncke, K.D., K. Fehsel, and V. Kolb-Bachofen, *Nitric oxide: cytotoxicity versus cytoprotection--how, why, when, and where?* Nitric Oxide, 1997. **1**(2): p. 107-20.
138. Bolanos, J.P., et al., *Nitric oxide-mediated mitochondrial damage in the brain: mechanisms and implications for neurodegenerative diseases*. J Neurochem, 1997. **68**(6): p. 2227-40.
139. Wheeler, M.A., et al., *Bacterial infection induces nitric oxide synthase in human neutrophils*. J Clin Invest, 1997. **99**(1): p. 110-6.
140. Molina y Vedia, L., et al., *Nitric oxide-induced S-nitrosylation of glyceraldehyde-3-phosphate dehydrogenase inhibits enzymatic activity and increases endogenous ADP-ribosylation*. J Biol Chem, 1992. **267**(35): p. 24929-32.
141. Gopalakrishna, R., Z.H. Chen, and U. Gundimeda, *Nitric oxide and nitric oxide-generating agents induce a reversible inactivation of protein kinase C activity and phorbol ester binding*. J Biol Chem, 1993. **268**(36): p. 27180-5.
142. Schlossmann, J., R. Feil, and F. Hofmann, *Signaling through NO and cGMP-dependent protein kinases*. Ann Med, 2003. **35**(1): p. 21-7.
143. Brune, B., A. von Knethen, and K.B. Sandau, *Nitric oxide (NO): an effector of apoptosis*. Cell Death Differ, 1999. **6**(10): p. 969-75.
144. Schafer, F.Q., et al., *Comparing beta-carotene, vitamin E and nitric oxide as membrane antioxidants*. Biol Chem, 2002. **383**(3-4): p. 671-81.
145. Frank, S., et al., *Nitric oxide drives skin repair: novel functions of an established mediator*. Kidney Int, 2002. **61**(3): p. 882-8.
146. Liebmann, J., M. Born, and V. Kolb-Bachofen, *Blue-light irradiation regulates proliferation and differentiation in human skin cells*. J Invest Dermatol, 2010. **130**(1): p. 259-69.
147. Yamasaki, K., et al., *Reversal of impaired wound repair in iNOS-deficient mice by topical adenoviral-mediated iNOS gene transfer*. J Clin Invest, 1998. **101**(5): p. 967-71.
148. Benrath, J., M. Zimmermann, and F. Gillardon, *Substance P and nitric oxide mediate wound healing of ultraviolet photodamaged rat skin: evidence for an effect of nitric oxide on keratinocyte proliferation*. Neurosci Lett, 1995. **200**(1): p. 17-20.
149. Stallmeyer, B., et al., *The function of nitric oxide in wound repair: inhibition of inducible nitric oxide-synthase severely impairs wound reepithelialization*. J Invest Dermatol, 1999. **113**(6): p. 1090-8.
150. Broughton, G., 2nd, J.E. Janis, and C.E. Attinger, *The basic science of wound healing*. Plast Reconstr Surg, 2006. **117**(7 Suppl): p. 12s-34s.

## References

151. Schaffer, M.R., et al., *Nitric oxide metabolism in wounds*. J Surg Res, 1997. **71**(1): p. 25-31.
152. Seabra, A.B., et al., *Topically applied S-nitrosothiol-containing hydrogels as experimental and pharmacological nitric oxide donors in human skin*. Br J Dermatol, 2004. **151**(5): p. 977-83.
153. Schwentker, A., et al., *Nitric oxide and wound repair: role of cytokines?* Nitric Oxide, 2002. **7**(1): p. 1-10.
154. Efron, D.T., D. Most, and A. Barbul, *Role of nitric oxide in wound healing*. Curr Opin Clin Nutr Metab Care, 2000. **3**(3): p. 197-204.
155. Stone, J.R. and S. Yang, *Hydrogen Peroxide: A Signaling Messenger*. Antioxidants & Redox Signaling, 2006. **8**(3-4): p. 243-270.
156. Lennicke, C., et al., *Hydrogen peroxide - production, fate and role in redox signaling of tumor cells*. Cell Commun Signal, 2015. **13**: p. 39.
157. Apel, K. and H. Hirt, *Reactive oxygen species: metabolism, oxidative stress, and signal transduction*. Annu Rev Plant Biol, 2004. **55**: p. 373-99.
158. Armstrong, D.A. and J.D. Buchanan, *Reactions of O<sub>2</sub><sup>-2</sup>, H<sub>2</sub>O<sub>2</sub> and other oxidants with sulfhydryl enzymes*. Photochem Photobiol, 1978. **28**(4-5): p. 743-55.
159. Arnold, R.S., et al., *Hydrogen peroxide mediates the cell growth and transformation caused by the mitogenic oxidase Nox1*. Proc Natl Acad Sci U S A, 2001. **98**(10): p. 5550-5.
160. Wang, Y., et al., *Superoxide dismutases: Dual roles in controlling ROS damage and regulating ROS signaling*. Journal of Cell Biology, 2018. **217**(6): p. 1915-1928.
161. Zito, E., *ERO1: A protein disulfide oxidase and H<sub>2</sub>O<sub>2</sub> producer*. Free Radical Biology and Medicine, 2015. **83**: p. 299-304.
162. Wong, H.S., et al., *Production of superoxide and hydrogen peroxide from specific mitochondrial sites under different bioenergetic conditions*. J Biol Chem, 2017. **292**(41): p. 16804-16809.
163. *Carcinogenesis and Reactive Oxygen Species Signaling: Interaction of the NADPH Oxidase NOX1–5 and Superoxide Dismutase 1–3 Signal Transduction Pathways*. Antioxidants & Redox Signaling, 2019. **30**(3): p. 443-486.
164. Hanschmann, E.M., et al., *Thioredoxins, glutaredoxins, and peroxiredoxins--molecular mechanisms and health significance: from cofactors to antioxidants to redox signaling*. Antioxid Redox Signal, 2013. **19**(13): p. 1539-605.
165. Griendling, K.K., D. Sorescu, and M. Ushio-Fukai, *NAD(P)H oxidase: role in cardiovascular biology and disease*. Circ Res, 2000. **86**(5): p. 494-501.
166. Babior, B.M., R.S. Kipnes, and J.T. Curnutte, *Pillars article: Biological defense mechanisms. The production by leukocytes of superoxide, a potential bactericidal agent*. J. Clin. Invest. 1973. 52: 741-744. J Immunol, 2014. **193**(11): p. 5359-62.
167. Meier, B., et al., *Human fibroblasts release reactive oxygen species in response to interleukin-1 or tumour necrosis factor-alpha*. Biochem J, 1989. **263**(2): p. 539-45.
168. Loschen, G., L. Flohe, and B. Chance, *Respiratory chain linked H(2)O(2) production in pigeon heart mitochondria*. FEBS Lett, 1971. **18**(2): p. 261-264.
169. Loschen, G., et al., *Superoxide radicals as precursors of mitochondrial hydrogen peroxide*. FEBS Lett, 1974. **42**(1): p. 68-72.
170. Drose, S. and U. Brandt, *The mechanism of mitochondrial superoxide production by the cytochrome bc1 complex*. J Biol Chem, 2008. **283**(31): p. 21649-54.
171. Siebels, I. and S. Drose, *Q-site inhibitor induced ROS production of mitochondrial complex II is attenuated by TCA cycle dicarboxylates*. Biochim Biophys Acta, 2013. **1827**(10): p. 1156-64.
172. Benhar, M., *Roles of mammalian glutathione peroxidase and thioredoxin reductase enzymes in the cellular response to nitrosative stress*. Free Radic Biol Med, 2018. **127**: p. 160-164.

## References

173. Detienne, G., et al., *Beyond ROS clearance: Peroxiredoxins in stress signaling and aging*. Ageing Res Rev, 2018. **44**: p. 33-48.
174. Keilin, D. and E.F. Hartree, *Properties of catalysis of coupled oxidation of alcohols*. Biochem J, 1945. **39**(4): p. 293-301.
175. Sies, H., *Role of metabolic H<sub>2</sub>O<sub>2</sub> generation: redox signaling and oxidative stress*. J Biol Chem, 2014. **289**(13): p. 8735-41.
176. Poole, L.B., *The basics of thiols and cysteines in redox biology and chemistry*. Free Radical Biology and Medicine, 2015. **80**: p. 148-157.
177. Antunes, F. and P.M. Brito, *Quantitative biology of hydrogen peroxide signaling*. Redox Biol, 2017. **13**: p. 1-7.
178. *Thioredoxins, Glutaredoxins, and Peroxiredoxins—Molecular Mechanisms and Health Significance: from Cofactors to Antioxidants to Redox Signaling*. Antioxidants & Redox Signaling, 2013. **19**(13): p. 1539-1605.
179. Xiao, Z., et al., *Molecular Mechanisms of Glutaredoxin Enzymes: Versatile Hubs for Thiol–Disulfide Exchange between Protein Thiols and Glutathione*. Journal of Molecular Biology, 2019. **431**(2): p. 158-177.
180. van der Vliet, A. and Y.M. Janssen-Heininger, *Hydrogen peroxide as a damage signal in tissue injury and inflammation: murderer, mediator, or messenger?* J Cell Biochem, 2014. **115**(3): p. 427-35.
181. Marinho, H.S., et al., *Hydrogen peroxide sensing, signaling and regulation of transcription factors*. Redox Biol, 2014. **2**: p. 535-62.
182. Niethammer, P., et al., *A tissue-scale gradient of hydrogen peroxide mediates rapid wound detection in zebrafish*. Nature, 2009. **459**(7249): p. 996-9.
183. Graham, K.A., et al., *NADPH oxidase 4 is an oncoprotein localized to mitochondria*. Cancer Biol Ther, 2010. **10**(3): p. 223-31.
184. Laurindo, F.R., T.L. Araujo, and T.B. Abrahao, *Nox NADPH oxidases and the endoplasmic reticulum*. Antioxid Redox Signal, 2014. **20**(17): p. 2755-75.
185. Marschall, R. and P. Tudzynski, *Reactive oxygen species in development and infection processes*. Semin Cell Dev Biol, 2016. **57**: p. 138-146.
186. Loo, A.E., R. Ho, and B. Halliwell, *Mechanism of hydrogen peroxide-induced keratinocyte migration in a scratch-wound model*. Free Radic Biol Med, 2011. **51**(4): p. 884-92.
187. Loo, A.E. and B. Halliwell, *Effects of hydrogen peroxide in a keratinocyte-fibroblast co-culture model of wound healing*. Biochem Biophys Res Commun, 2012. **423**(2): p. 253-8.
188. Loo, A.E., et al., *Effects of hydrogen peroxide on wound healing in mice in relation to oxidative damage*. PLoS One, 2012. **7**(11): p. e49215.
189. Eligini, S., et al., *Cyclooxygenase-2 mediates hydrogen peroxide-induced wound repair in human endothelial cells*. Free Radic Biol Med, 2009. **46**(10): p. 1428-36.
190. Cho, M., T.K. Hunt, and M.Z. Hussain, *Hydrogen peroxide stimulates macrophage vascular endothelial growth factor release*. Am J Physiol Heart Circ Physiol, 2001. **280**(5): p. H2357-63.
191. Ito, J., et al., *Enhancement of FGF-1 release along with cytosolic proteins from rat astrocytes by hydrogen peroxide*. Brain Res, 2013. **1522**: p. 12-21.
192. Wilgus, T.A., et al., *Hydrogen peroxide disrupts scarless fetal wound repair*. Wound Repair Regen, 2005. **13**(5): p. 513-9.
193. De Deken, X., et al., *Roles of DUOX-mediated hydrogen peroxide in metabolism, host defense, and signaling*. Antioxid Redox Signal, 2014. **20**(17): p. 2776-93.
194. Golda, J., et al., *Concepts and characteristics of the 'COST Reference Microplasma Jet'*. Journal of Physics D-Applied Physics, 2016. **49**(8).
195. Sellers, R.M., *Spectrophotometric determination of hydrogen peroxide using potassium titanium(IV) oxalate*. Analyst, 1980. **105**(1255): p. 950-954.

## References

196. Suschek, C.V., C. Oplander, and E.E. van Faassen, *Non-enzymatic NO production in human skin: effect of UVA on cutaneous NO stores*. Nitric Oxide, 2010. **22**(2): p. 120-35.
197. Heuer, K., et al., *The topical use of non-thermal dielectric barrier discharge (DBD): nitric oxide related effects on human skin*. Nitric Oxide, 2015. **44**: p. 52-60.
198. van Faassen, E.E., et al., *Nitrite as regulator of hypoxic signaling in mammalian physiology*. Medicinal research reviews, 2009. **29**(5): p. 683-741.
199. Oplander, C., et al., *Characterization of novel nitrite-based nitric oxide generating delivery systems for topical dermal application*. Nitric Oxide, 2013. **28**: p. 24-32.
200. Zemke, A.C., et al., *Nitrite modulates bacterial antibiotic susceptibility and biofilm formation in association with airway epithelial cells*. Free Radic Biol Med, 2014. **77**: p. 307-16.
201. Schlag, S., et al., *Inhibition of staphylococcal biofilm formation by nitrite*. J Bacteriol, 2007. **189**(21): p. 7911-9.
202. Weller, R., et al., *Antimicrobial effect of acidified nitrite on dermatophyte fungi, Candida and bacterial skin pathogens*. J Appl Microbiol, 2001. **90**(4): p. 648-52.
203. Ormerod, A.D., et al., *An observational prospective study of topical acidified nitrite for killing methicillin-resistant Staphylococcus aureus (MRSA) in contaminated wounds*. BMC Res Notes, 2011. **4**: p. 458.
204. Oehmigen, K., et al., *The Role of Acidification for Antimicrobial Activity of Atmospheric Pressure Plasma in Liquids*. Plasma Processes and Polymers, 2010. **7**(3-4): p. 250-257.
205. Mammone, T., M. Ingrassia, and E. Goyarts, *Osmotic stress induces terminal differentiation in cultured normal human epidermal keratinocytes*. In Vitro Cell Dev Biol Anim, 2008. **44**(5-6): p. 135-9.
206. Hashimoto, S., et al., *Hyperosmolarity-induced interleukin-8 expression in human bronchial epithelial cells through p38 mitogen-activated protein kinase*. Am J Respir Crit Care Med, 1999. **159**(2): p. 634-40.
207. van Gils, C.A.J., et al., *Mechanisms of bacterial inactivation in the liquid phase induced by a remote RF cold atmospheric pressure plasma jet*. Journal of Physics D: Applied Physics, 2013. **46**(17): p. 175203.
208. Tian, W. and M.J. Kushner, *Atmospheric pressure dielectric barrier discharges interacting with liquid covered tissue*. Journal of Physics D: Applied Physics, 2014. **47**(16): p. 165201.
209. Winter, J., et al., *Tracking plasma generated H<sub>2</sub>O<sub>2</sub> from gas into liquid phase and revealing its dominant impact on human skin cells*. Journal of Physics D: Applied Physics, 2014. **47**(28): p. 285401.
210. Balzer, J., et al., *Non-Thermal Dielectric Barrier Discharge (DBD) Effects on Proliferation and Differentiation of Human Fibroblasts Are Primary Mediated by Hydrogen Peroxide*. PLoS One, 2015. **10**(12): p. e0144968.
211. Chen, Q. and B.N. Ames, *Senescence-like growth arrest induced by hydrogen peroxide in human diploid fibroblast F65 cells*. Proceedings of the National Academy of Sciences of the United States of America, 1994. **91**(10): p. 4130-4134.
212. Hoffmanns, M.A., et al., *Acidification and Nitrite/Nitrate Accumulation by Nonthermal Dielectric Barrier Discharge (DBD) Affect Human Dermal Fibroblasts*. Plasma Medicine, 2015. **5** (1): p. 71-85.
213. Barekzi, N. and M. Laroussi, *Effects of Low Temperature Plasmas on Cancer Cells*. Plasma Processes and Polymers, 2013. **10**(12): p. 1039-1050.
214. Lee, S.Y., et al., *Nonthermal plasma induces apoptosis in ATC cells: involvement of JNK and p38 MAPK-dependent ROS*. Yonsei medical journal, 2014. **55**(6): p. 1640-1647.
215. Golda, J., et al., *Concepts and characteristics of the 'COST Reference Microplasma Jet'*. Journal of Physics D: Applied Physics, 2016. **49**(8): p. 084003.
216. Kelly, S., et al., *Gas and heat dynamics of a micro-scaled atmospheric pressure plasma reference jet*. Journal of Physics D: Applied Physics, 2015. **48**(44): p. 444002.

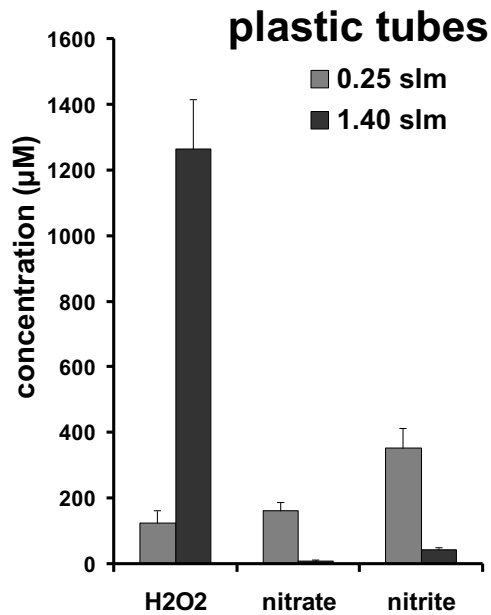
## 7. Acknowledgment

I thank Samira Seghrouchni, Christa-Maria-Wilkens, and Jutta Schneider for technical assistance.

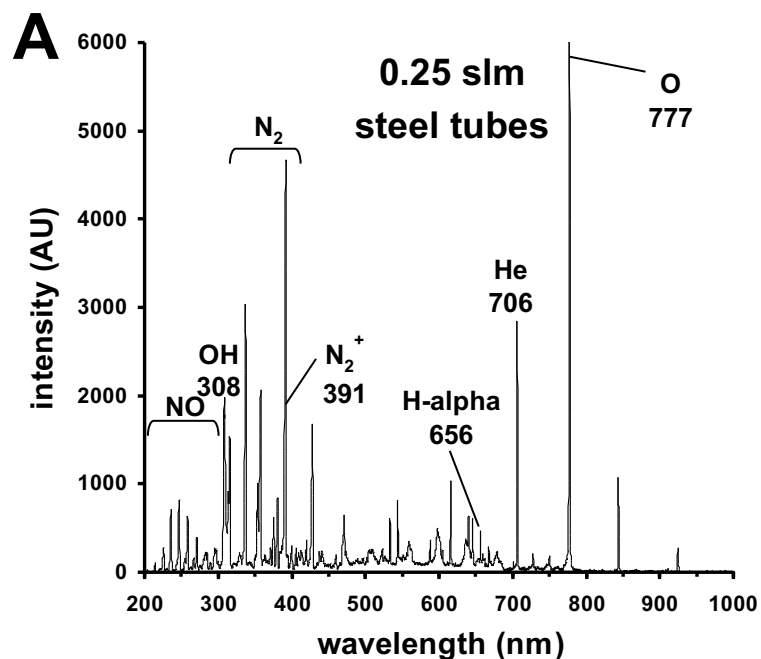
I am particularly grateful for everyone who supported me so wonderfully. Above all my family and dearest friends.

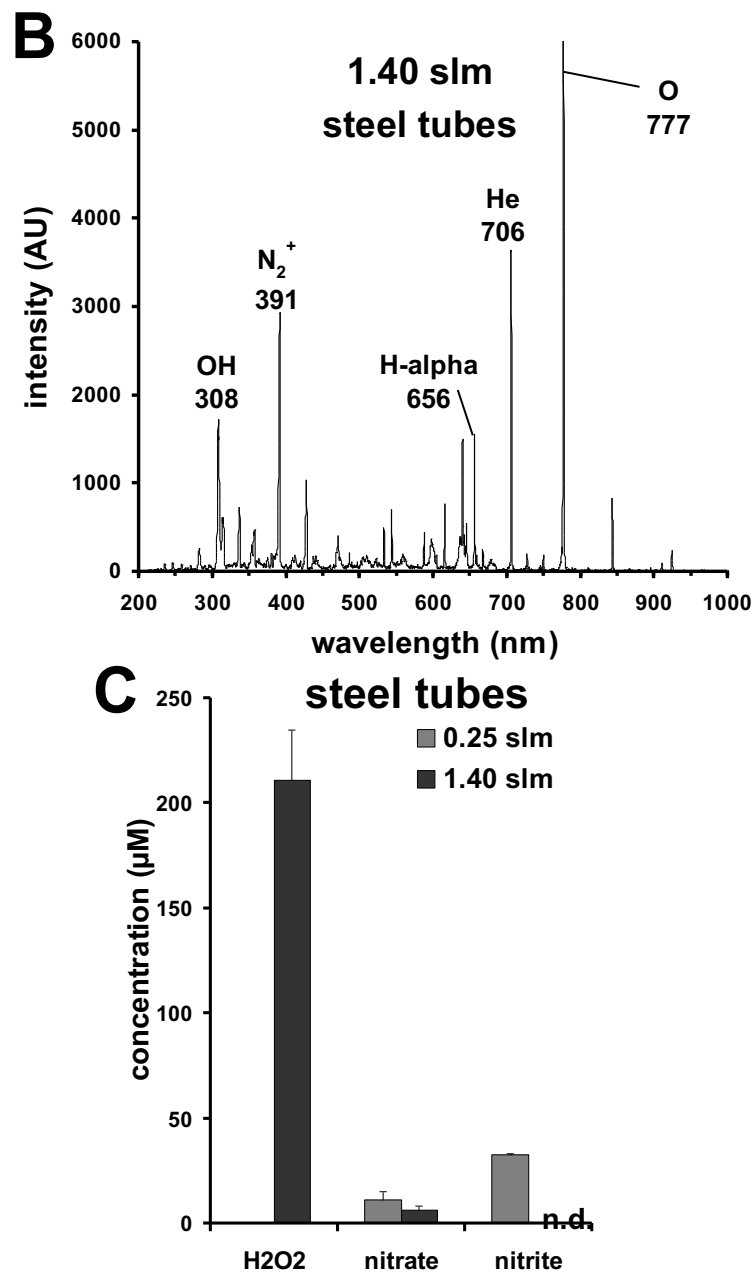
## 8. Supplement material

### 8.1 Material of gas delivery system affects OEC spectra and CAP-induced accumulation of hydrogen peroxide, nitrite and nitrate



*Supplement Figure 1 CAP characterization under plastic tube feed. Shown are the OES- spectra of plasma generated by  $\mu$ APP jet at a gas flow of 0.25 slm (A) and 1.4 slm (B) using plastic tubes for gas delivery. The obtained hydrogen peroxide, nitrite and nitrate concentration after 10 min CAP treatment of 500  $\mu$ l PBS under these conditions are shown in C.*





**Supplement Figure II CAP characterization under steel tube feed.** Shown are the OES- spectra of plasma generated by  $\mu\text{APP}$  jet at a gas flow of 0.25 slm (A) and 1.4 slm (B) using steel tubes for gas delivery. The obtained hydrogen peroxide, nitrite and nitrate concentration after 10 min CAP treatment of 500  $\mu\text{l}$  PBS under these conditions are shown in C.